Electrocoagulation process in water treatment: A review of electrocoagulation modeling approaches

Jean Nepo Hakizimana [a,f], Bouchaib Gourich [a,*], Mohammed Chafi [a], Youssef Stiriba [b], Christophe Vial [c,d], Patrick Drogui [e], Jamal Naja [f]

[a] Laboratoire d'Environnement, Procédés et Energie, Ecole Supérieure de Technologie, Université Hassan II de Casablanca, Route d'El Jadida, km 7, BP 8012, Oasis Casablanca, Morocco
[b] ETSEQ, Departament d'Enginyeria Mecanica, Universitat Rovira i Virgili, Av. Països Catalans 26, 43007 Tarragona, Spain
[c] Université Clermont Auvergne, Université Blaise Pascal, Institut Pascal, BP 10448, F-63000 Clermont-Ferrand, France
[d] CNRS, UMR 6602, IP, F-63178 Aubière, France
[e] Laboratoire d'Electrotechnologies Environnementales et Procédés Oxydatifs (LEEPO), Centre Eau Terre Environnement, Institut National de la Recherche Scientifique (INRS), 490, rue de la Couronne, Québec (Québec) G1K 9A9, Canada
[f] Chimie Appliquée et Environnement, Faculté des Sciences et Techniques Settat, B.P 577 Route de Casablanca, Morocco

HIGHLIGHTS

• Electrocoagulation is a versatile process able to treat drinking and waste waters.
• The pros and cons of electrocoagulation (EC) are compared to alternative processes.
• EC suffers from a lack of scale-up methodology and the current models are reviewed.
• Four challenges emerge, covering theoretical, modeling and techno-economic aspects.
• Outlooks for future research and developments are suggested.

ARTICLE INFO

ABSTRACT

Electrocoagulation process (EC) has been the subject of several reviews in the last decade, and is still a very active area of research. Most published works deals with applications for treatment of drinking water and urban, industrial or agricultural wastewaters so as to enhance the simultaneous abatement of soluble and colloidal pollution. These also include contributions to theoretical understanding, electrode materials, operating conditions, reactor design and even techno-economic analysis. Even though, the numerous advantages reported in the literature, and the pros and cons of EC in comparison to alternative processes, its industrial application is not yet considered as an established wastewater technology because of the lack of systematic models for reactor scale-up. This paper presents a comprehensive review on its development and design. The most recent advances on EC reactor modeling are summarized with special emphasis on four major issues that still constitute the cornerstone of EC: the theoretical understanding of mechanisms governing pollution abatement, modeling approaches, CFD simulations, and techno-economic optimization. Finally, outlooks for future research and developments are suggested.

© 2016 Elsevier B.V. All rights reserved.

Contents

* Corresponding author.
    E-mail address: gourichgp@hotmail.com (B. Gourich).

1. Introduction

Preservation of water resources is one of the 21st century's biggest challenges. It has to face several issues, which among them are: population growth, deforestation, rapid urbanization, industrialization and warming global climate change [1]. Nowadays, the access to safe drinking water is limited and under stress; water pollution may seriously impact aquatic ecosystems and the availability of healthy freshwater. Therefore, there is a need to develop efficient technologies and approaches for treating and managing wastewaters, to maintain quality and improve quantity at large scale while ensuring environmental protection and sustainability, for instance urban, industrial and agricultural wastewaters. More robust efficient drinking water treatments are also required to deal with risks posed by environmental contamination, for example presence of nitrate or fluoride ions at high concentrations.

The EC process can be used for the treatment of drinking water and wastewater. EC consists of generating coagulant species in situ by electrolytic oxidation of sacrificial anode materials triggered by electric current applied through the electrodes. The metal ions generated by electrochemical dissolution of a consumable anode spontaneously undergo hydrolysis in water, depending on the pH, forming various coagulant species including hydroxide precipitates (able to remove pollutants by adsorption/settling) and other ions metal species. Al and Fe materials are the most commonly used as electrode materials thanks to various advantages: their availability, i.e. abundance on the earth and low price, their non-toxicity, as iron and aluminum hydroxides formed by precipitation are relatively non-toxic, and their high valence that leads to an efficient removal of pollutant. Besides, simultaneous cathodic reaction allows for pollutant removal either by deposition on cathode electrode or by flotation (evolution of hydrogen at the cathode). The anode and the cathode are usually made of the same metal, although electrodissolution should occur only at the anode. EC can be conducted as a batch or continuous process. The large extent of its applications has been recently reviewed by Emamjomeh and Sivakumar [2] and more recently by Kabdaşh et al. [3]. EC is an old process, as old as electricity [3]. The use of EC in drinking water treatment plants was reported in the 19th century in England and wastewater treatment plants operated in the USA in the beginning of the 20th century [4]. At the end of the 30s, it had been mainly replaced by chemical coagulation and by biological treatments for the abatement of colloidal and soluble organic pollutions in wastewater, respectively. The main reason was the higher operating cost, in particular the price of electricity in this period. The situation has, of course, drastically changed and the advantages of EC have been "rediscovered" since the 90s. Mollah et al. [5] have reported 10 advantages that have been, more or less, assessed in the literature. These can be summarized in Table 1, with the specific drawbacks of EC in comparison to alternative treatments. EC presents also other issues than cited in Table 1, for example the need for sludge handling, but chemical coagulation and activated sludge process have to address the same issue. In practice, the composition of EC sludge is close to that obtained using chemical coagulation when either alum or ferric chloride are used, which means that sludge disposal should be similar. Conversely, a specific issue of EC is that, to the best of our knowledge, there are unfortunately almost no comprehensive reviews of EC modeling and scale-up approaches for water treatment.

The aim of this work is, therefore, to summarize, discuss and analyze recent advances on modeling approaches developed for the simulation and the scale-up of EC operation. We start first by describing various mechanisms for pollution abatement. Then, the key operation parameters and reactor design attributes will be discussed so as to introduce the details of modeling aspects. Later, the main methodologies and design strategies will be reviewed from a critical point of view and linked to the techno-economic analysis of the EC process. Finally, some outlooks for future research and developments will be suggested.

2. Theoretical background on electrocoagulation process

Electrocoagulation combines various mechanisms that can be electrochemical (metal dissolution and water reduction, pollutant electro-oxidation or electro-reduction…), chemical (acid/base equilibria with pH change, hydroxide precipitation, redox reaction in the bulk…) and physical (physical adsorption, coagulation, flotation…). These can be sequential and/or parallel. All of them are summarized in Fig. 1 which highlights the complexity and the interplay between the mechanisms of EC process. These mechanisms are detailed below.

Table 1
The advantages and disadvantages of the EC process.

| Advantages	Disadvantages
Nonspecific method	Need for maintenance
Address drinking water and wastewater	
Combines oxidation, coagulation and precipitation (results in lower capital costs [5])	Electrode passivation over time
Reduced need for chemical reagents (replaced by either Al or Fe electrodes and electricity)	Need for high-conductivity water
Reduced operating cost	
Reduced risk of secondary pollution	
Low sludge production	Lack of systematic reactor design [4]
Without moving parts	
Low energy requirements	
Solar power can be used	
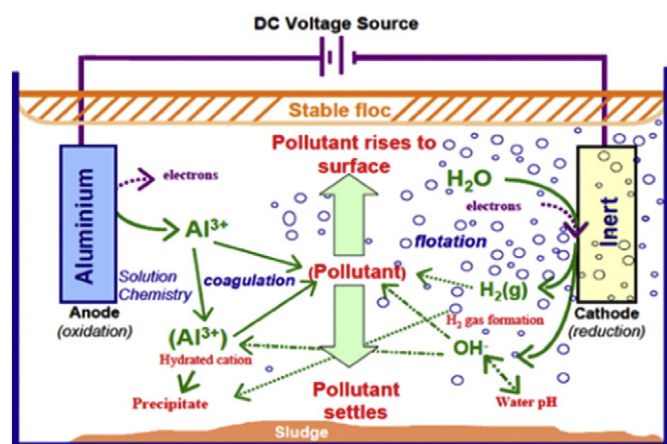
Fig. 1. Interactions occurring within EC reactor [6] (although on this figure, there is an inert cathode, in discussion, the cathode has been often considered made of the same material as the anode to explain chemical dissolution).
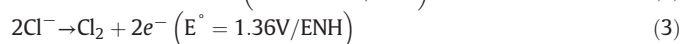
2.1. Electrocoagulation mechanisms

In the EC process, coagulant species are generated in situ using the electrodissolution of a sacrificial anode, usually in iron or aluminum, using by electric current applied between metal electrodes.

Chemical reactions can be summarized as follows:

• At the anode, metal is oxidized into cations

$$M \rightarrow M^{Z+} + Ze^- \tag{1}$$

In this equation, Z is the number of electrons transferred in the anodic dissolution process per mole of metal. In the case of high anode potential, secondary reactions may occur [7,8]. Water may be oxidized and leads to hydronium cation and oxygen gas and in the presence of chloride anions, Cl^- may be oxidized into Cl_2. The latter being a strong oxidant may contribute to the oxidation of dissolved organic compounds or may lead to the formation of ClOH that also plays the role of oxidizer [9].

$$2H_2O \rightarrow O_2 + 4H^+ + 4e^- \left(E^\circ = 1.23\ V/ENH\right) \tag{2}$$

$$2Cl^- \rightarrow Cl_2 + 2e^- \left(E^\circ = 1.36V/ENH\right) \tag{3}$$

$$Cl_2 + H_2O \rightarrow ClOH + Cl^- + H^+ \tag{4}$$

• At the cathode: water is reduced into hydrogen gas and hydroxyl anions

$$3H_2O + 3e^- \rightarrow \frac{3}{2}H_2 + 3OH^- \left(E^\circ = 0.00V/ENH\right) \tag{5}$$
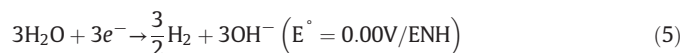
The amount of metal dissolved by anodic oxidization can be calculated using Faraday's law (Eq. (6)). The mass of metal m is, therefore, a function of the electrolysis time t and of the electric current I:

$$m = \phi \frac{It}{ZF} M \tag{6}$$

In Eq. (6), M is the atomic weight of the electrode material, and F is Faraday's constant. However, Faraday's law ($\phi = 1$) is valid only when all the electrons in the system participate only in the metal-dissolution reaction at the anode. When parallel reactions occur, a correction factor, denoted *current efficiency* or *faradic yield* (ϕ), is used to account for the gap between the theoretical and experimental dissolution of the sacrificial anode [10,11]. This value is usually lower than 1 [12], but ϕ may be higher than 1 when the chemical and the electrochemical oxidation mechanisms of the metal proceed simultaneously. This last situation is frequent with aluminum [13,14]. The metal cations released in the bulk undergo various equilibrium reactions that correspond to acid/base, complexation, precipitation and redox reactions in water. The role of these removal mechanisms depends on pollutant species, as illustrated in Table 2.

However, for the metal cations released from the anode, the most common phenomenon is the formation of metal hydroxides that exhibit poor solubility and readily precipitate. As a result, water soluble pollutants may also adsorb physically or chemically onto the precipitates. Alternative pollution abatement mechanisms involve:

• The purely physical enmeshment of dissolved substances during hydroxide precipitation, adsorption and complexation. For instance, phosphates are removed from effluents by complexation and/or by precipitation with metallic hydroxides and/or by adsorption on the latter while the dissolved organic compound removal from wastewaters can be attributed to the co-precipitation and/or to complexation and/or to electrostatic attraction on the surface of metallic hydroxides. For the complexation, the pollutant can act as a ligand (L) to bind a hydrous iron moiety or aluminum hydroxides (see Eqs. (7) and (8)):

$$L-H_{(aq)} + (OH)OFe_{(s)} \rightarrow L-OFe_{(s)} + H_2O \tag{7}$$

$$L-H_{(aq)} + (OH)(OH)_2Al_{(s)} \rightarrow L-(OH)_2Al_{(s)} + H_2O \tag{8}$$
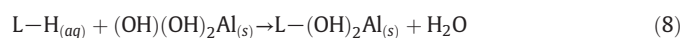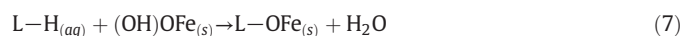
Table 2
Equilibrium reactions of metal hydroxides with soluble pollutants in the bulk.

Soluble pollutants	Mechanism of abatement	References
Sulfide anions	Precipitation	[15]
Calcium cations	Co-precipitation	[16]
Phosphate anions	Precipitation, adsorption, complexation	[17,18]
Organic compounds	Complexation, co-precipitation	[19]
Fluoride anions	Complexation, precipitation	[20,21]
Arsenate anions		[22]

Fig. 2. Main mechanisms of soluble pollution abatement using EC.

- The electro-oxidation on the anode or the electro-reduction on the cathode of electro-active ions or molecules, such as the reduction of cationic Cr(VI) into Cr(III) cations followed by Cr(III) hydroxide precipitation [23], the reduction of ani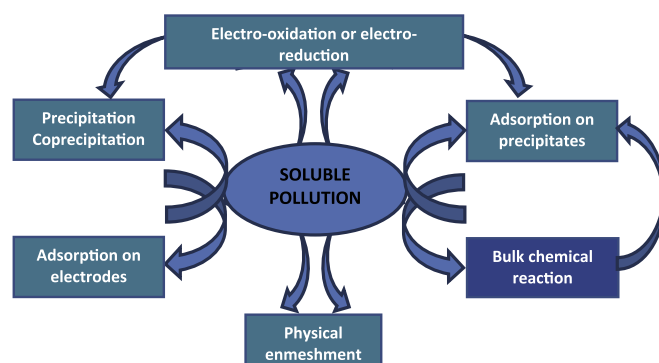onic nitrates into nitrite, ammonia and nitrogen gas [24] and the oxidation instead of reduction when trivalent arsenic As(III) is oxidized into pentavalent arsenic As(V) [25]. Some authors have reported that heavy metals may also undergo electro-reduction at the cathode surface during the EC process [26].
- The direct adsorption of pollutants on the electrodes: especially for fluoride anions due to the electro-condensation where the fluoride anions are attracted to the anode by the electric forces [20,27].

These mechanisms for soluble pollutants are summarized in Fig. 2. In practice, there is usually a prevailing mechanism for each pollutant which is a function of the nature of this pollutant. Typical examples are summarized in Table 2 and more details can be found in review papers on EC [2–3].

In parallel, colloidal suspensions and emulsions are also destabilized by the continuous coagulant dosing from electrochemical dissolution as in chemical coagulation [28]. The tendency of particles to coagulate or to remain discrete and dispersed results from the net inter-particles force that is predicted by the sum of opposing forces between the attractive van der Waals and the repulsive forces of the electrical double-layer as defined by the DLVO theory as a first approximation [29]. The destabilization mechanisms are summarized as follows:

- The compression of the double layer of a colloidal particle is caused by interactions with the soluble ionic species generated from electrochemical dissolution of the sacrificial electrodes. This affects electrical potential difference between the particle surface and the bulk solution and results in reducing the repulsive forces between particles [30].
- Charge neutralization is performed by adsorption of ionic metal species/hydronium cations/hydroxyl anions or by the precipitation of charged hydroxide precipitates onto the surface of charged colloidal particles present in water/wastewater [31]. This could be indicated by an evolution of the zeta potential around the isoelectric point.
- Colloids entrapment (enmeshment mechanism or sweep coagulation): hydroxide precipitates entrap the colloidal particles that are in water/wastewater. This destabilization mechanism depends on metal hydroxide precipitates that can be formed [31]. This mechanism prevails about neutral pH.

Throughout the EC process, these destabilization mechanisms summarized in Fig. 3 may take place simultaneously or consecutively according to the features of the water/wastewater to treat, the pollutants to be removed, the operating conditions (especially current), and the nature of the metal. Contrary to soluble pollutants, the
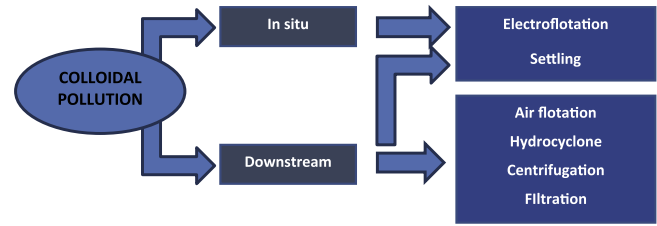
Fig. 3. Main mechanisms of insoluble colloidal pollution abatement using EC.

Fig. 4. Main mechanisms of EC sludge removal.

prevailing mechanism is, therefore, more difficult to define a priori because it is often more dependent on operating conditions than on the nature of the particles. Thereafter, the destabilization step is followed by flocculation that consists of aggregation of the coagulated particles and the precipitates [32]. Flocculation efficiency depends on the success of the destabilization phase and the collision rate of particles [30].

As the abatement of soluble species involves adsorption and enmeshment, the mechanisms of soluble and colloidal substances are intrinsically linked. The flocculated contaminants, forming EC sludge, can then be removed from water by physical method, in situ or using a downstream process, as shown in Fig. 4. In situ, the two main methods involve electroflotation and settling. Settling and electroflotation can also be used as downstream treatments, but in this case, other downstream treatments are available for sludge removal including filtration, centrifugation, hydrocycloning, and flotation, in particular dissolved air flotation.

2.2. Specificity of Al electrodes

For aluminum, only the half-oxidation reaction between Al^{3+}/Al follows Eq. (1), as $Z = 3$. In addition to the reactions described in Section 2.1, other monomeric species are formed from the spontaneous hydrolysis of Al^{3+} cations according to the acid/base reactions (Eqs. (9)–(12)) and Al^{3+} concentration [8,33].

$$Al^{3+} + H_2O \rightarrow Al(OH)^{2+} + H^+ \tag{9}$$

$$Al(OH)^{2+} + H_2O \rightarrow Al(OH)_2^+ + H^+ \tag{10}$$

$$Al(OH)_2^+ + H_2O \rightarrow Al(OH)_3 + H^+ \tag{11}$$

$$Al(OH)_3 + H_2O \rightarrow Al(OH)_4^- + H^+ \tag{12}$$

Aluminum speciation and partition can be deduced from E-pH Pourbaix diagrams when reactions are under thermodynamic control. This can be deduced from the equilibrium constants for acid/base reactions and standard reduction potentials summarized in Table 3.

In practice, soluble Al^{3+} cations prevail when pH is lower than 4, soluble aluminate anions prevail when pH is higher than 10, while the insoluble $Al(OH)_3$ form predominates otherwise. The formation of
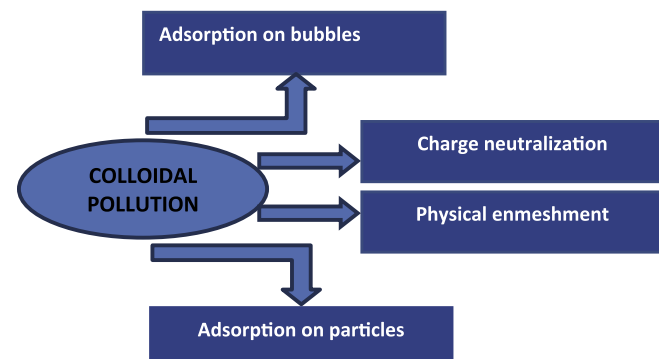
Table 3
Equilibrium constant and standard reduction potential of aluminum species.

Reaction	pK
$Al^{3+}_{(aq)} + H_2O = Al(OH)^{2+}_{(aq)} + H^+_{(aq)}$	4.997
$Al^{3+}_{(aq)} + 2H_2O = Al(OH)^+_{2\ (aq)} + 2H^+_{(aq)}$	10.094
$Al^{3+}_{(aq)} + 3H_2O = Al(OH)_{3\ (aq)} + 3H^+_{(aq)}$	16.791
$Al^{3+}_{(aq)} + 3H_2O = Al(OH)_{3\ (s)} + 3H^+_{(aq)}$ (amorphous)	8.578
$Al^{3+}_{(aq)} + 2H_2O = AlO(OH)_{(s)} + 3H^+_{(aq)}$ (boehmite)	10.800
$Al^{3+}_{(aq)} + 4H_2O = Al(OH)^-_{4\ (aq)} + 4H^+_{(aq)}$	22.688

Reaction	E° (V)
$Al^{3+}_{(aq)} + 3e^- = Al_{(s)}$	−0.41
$Fe^{3+}_{(aq)} + 3e^- = Fe_{(s)}$	−0.04
$Fe^{3+}_{(aq)} + 2e^- = Fe^{2+}_{(aq)}$	+0.77
$FeO_4^{2-}\ _{(aq)} + 3e^- + 8H^+ = Fe^{3+}_{(aq)} + 4H_2O$	+2.20

polymeric species has also been reported: $Al(OH)_{15}^{3+}, Al_7(OH)_{17}^{4+}$,-$Al_8(OH)_{20}^{4+}$ and $Al_{13}O_4(OH)_{24}^{7+}$. The Lewis acidity of aluminum counterbalances the formation of OH^- anions at the cathode, which induces a buffer effect and leads to a final pH between 7 and 8 which strongly differs from conventional chemical coagulation using Al salts [30]. As a result, monomeric and polymeric species induce finally the formation of the amorphous $Al(OH)_3$ "sweep flocs" which have large surface areas beneficial for a rapid adsorption of soluble organic compounds and trapping of colloidal particles [34–36].

$$nAl(OH)_3 \rightarrow Al_n(OH)_{3n} \tag{13}$$

Secondary reactions may occur at the electrodes due to a purely chemical attack of aluminum under acid or alkaline conditions, respectively [8,37]:

$$2Al + 6H^+ \rightarrow 2Al^{3+} + 3H_2 \tag{14}$$

$$2Al + 6H_2O + 2OH^- \rightarrow 2Al(OH)_4^- + 3H_2 \tag{15}$$
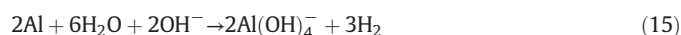
The consequence is that the amount of dissolved Al released during EC exceeds the expected concentration predicted by Faraday's law. The faradic yield ϕ is, therefore, higher than 100% and can reach 200% [8].

A key problem of EC process is the passivation of the cathode as it increases cell voltage and energy consumption. The passivation mechanism can be avoided by optimization of the current reversal frequency [38] or NaCl addition so as to promote pitting corrosion with a chemical reaction between Cl^- adsorbed on the aluminum oxide film with Al^{3+} species in the oxide lattice. The rate of chemical corrosion of soluble aluminum anodes depends mainly on two mechanisms [14]:

- The formation and build-up of a passive aluminum-oxide layer;
- The subsequent partial destruction of this layer through pitting.

The pitting corrosion depends strongly on the initial pH, the nature and the concentration of supporting electrolyte and the current density. The positive effect of anions on passive aluminum-oxide layer in the descending order [39] is: Cl^-, Br^-, I^-, F^-, ClO_4^-, OH^-, SO_4^{2-}. The pitting corrosion can largely affect the overall dissolution of sacrificial aluminum anode. The pitting potential E_{pit} (V) decreases with the logarithm of chloride concentration (ppm), as shown in Eq. (16) [8].

$$E_{pit} = 1.75 - 0.72 \cdot Ln[Cl^-] \tag{16}$$

Table 4
Equilibrium constant and standard reduction potential of iron species.

Reaction	pK
$Fe_{(aq)}^{2+} + H_2O = Fe(OH)_{(aq)}^+ + H_{(aq)}^+$	9.397
$Fe_{(aq)}^{2+} + 2H_2O = Fe(OH)_{2\ (aq)} + 2H_{(aq)}^+$	20.494
$Fe_{(aq)}^{2+} + 2H_2O = Fe(OH)_{2\ (s)} + 2H_{(aq)}^+$	13.564
$Fe_{(aq)}^{2+} + 2H_2O = Fe(OH)_{3\ (aq)}^- + 2H_{(aq)}^+$	28.991
$Fe_{(aq)}^{3+} + H_2O = Fe(OH)_{(aq)}^{2+} + H_{(aq)}^+$	2.187
$Fe_{(aq)}^{3+} + 2H_2O = Fe(OH)_{(aq)}^+ + 2H_{(aq)}^+$	4.594
$Fe_{(aq)}^{3+} + 3H_2O = Fe(OH)_3\ (aq) + 3H_{(aq)}^+$	12.56
$Fe_{(aq)}^{3+} + 2Fe_{(aq)}^{3+} + 8H_2O = Fe_3(OH)_{8\ (s)} + 8H_{(aq)}^+$	20.222
$Fe_{(aq)}^{3+} + 2H_2O = \alpha FeO(OH)_{(s)} + 3H_{(aq)}^+$	0.491
$Fe_{(aq)}^{3+} + 2H_2O = \gamma FeO(OH)_{(s)} + 3H_{(aq)}^+$	1.371
$Fe_{(aq)}^{3+} + 4H_2O = Fe(OH)_{4\ (aq)}^- + 4H_{(aq)}^+$	21.588
$2Fe_{(aq)}^{3+} + 2H_2O = Fe_2(OH)_{2\ (aq)}^{4+} + 2H_{(aq)}^+$	13.771
$3Fe_{(aq)}^{3+} + 4H_2O = Fe_3(OH)_{4\ (aq)}^{5+} + 4H_{(aq)}^+$	6.228

Reaction	E° (V)
$Fe_{(aq)}^{2+} + 2e^- = Fe_{(s)}$	−0.41
$Fe_{(aq)}^{3+} + 3e^- = Fe_{(s)}$	−0.04
$Fe_{(aq)}^{3+} + 2e^- = Fe_{(aq)}^{2+}$	+0.77
$FeO_{4\ (aq)}^{2-} + 3e^- + 8H^+ = Fe_{(aq)}^{3+} + 4H_2O$	+2.20

The mechanism of chemical dissolution induced by pitting corrosion in the presence of chloride ions may be expressed as follows [40]:

$$2Al + 6HCl \rightarrow 2AlCl_3 + 3H_2 \tag{17}$$

$$AlCl_3 + 3H_2O \rightarrow Al(OH)_3 + 3HCl \tag{18}$$
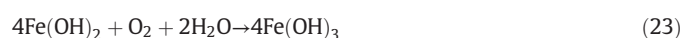
2.3. Specificity of iron electrodes

The electrochemical reactions taking place at iron electrodes or in aqueous medium during Fe-EC are more complex than with aluminum, as anode oxidation could lead either to ferrous or ferric cations:

$$Fe \rightarrow Fe^{2+} + 2e^- \tag{19}$$

$$Fe \rightarrow Fe^{3+} + 3e^- \tag{20}$$

Ferrous and ferric ions hydrolyze in water and form various monomeric and polymeric species whose proportions depend on the ferric ion concentration and on the pH: $Fe(OH)^{2+}, Fe(OH)_2^+, Fe(OH)_4^{2+}$,-$Fe(OH)_4^-, Fe(H_2O)_5(OH)^{2+}, Fe(H_2O)_4(OH)_2^+, Fe(H_2O)_8(OH)_2^{4+}$,-$Fe_2(H_2O)_6(OH)_4^{2+}$ and $Fe(OH)_3$. This complexity also emerges from Table 4 that summarizes the acid/base and equilibrium constants and standard reduction potentials of monomeric species.

Despite some ambiguities in various papers on the mechanism of Iron EC, recent studies usually assume that the anode oxidation releases Fe^{2+} because it has been proved that the dissolution rate of Fe^{3+} is negligible [41–43]. The oxidation of Fe^{2+} ions to Fe^{3+} ions depends strongly on pH and the dissolved oxygen concentration [41,44]. In acidic media, Fe^{2+} cations oxidize very slowly in contact with dissolved oxygen (Eq. (21)), while in neutral or alkaline media, Fe^{2+} is immediately transformed into ferrous hydroxide (Eq. (22)) which is quickly oxidized by dissolved oxygen to iron(III) hydroxide (Eq. (23)).

$$Fe^{2+} + O_2 + 2H_2O \rightarrow Fe^{3+} + 4OH^- \tag{21}$$

$$Fe^{2+} + 2OH^- \rightarrow Fe(OH)_2 \tag{22}$$

$$4Fe(OH)_2 + O_2 + 2H_2O \rightarrow 4Fe(OH)_3 \tag{23}$$

The consequence is that, on one hand, some studies report that the iron dissolution follows Faraday's law with a faradic yield between 80 and 100% [12,13,45]. On the other hand, others state that there is a difference between the amount of iron theoretically dissolved estimated by Faraday's law and the amount of observed dissolved iron based on $Z = 2$ [41]. In acidic media, ϕ is higher than 100%, whereas in alkaline media, the opposite is true. At lower pH values, possible explanations are similar to those reported for Al: chemical corrosion and pitting corrosion at both electrodes in the presence of some ionic compounds, such as chloride anions [41,45]. At higher pH values, the dissolution efficiency decreases below the Faraday's law values because secondary reactions occur near the anode, including oxygen evolution (Eq. (2)). For alkaline pH, iron oxidation leads to Fe(III) formation through Eq. (20) as oxide or hydroxide species. This decreases the iron concentration produced, because Fe(III) formation requires 3 electrons instead of 2 for Fe(II) and so, a higher current value for achieving the same iron concentration is required [41,42]. The various monomeric and polymeric species finally turn into amorphous $Fe(OH)_3$ precipitates that are efficient for a rapid adsorption of soluble organic compounds and trapping of colloidal particles [37,46].

Two other differences with Al electrodes can also be drawn. The first one is that the buffer effect reported for Fe is weaker than for Al. Final pH usually achieved is 9 or 10 with Fe electrodes even when the initial pH is acidic [44,47]. The second is that Fe^{2+} is highly soluble and therefore, not capable of an efficient colloid destabilization by $Fe(OH)_3$, hereby

causing poor EC performance [12]. Consequently, an efficient operation of Fe-EC requires one or more of the following optimization techniques for the Fe^{3+} production [41,44]:

(a) aerating the water to increase the dissolved oxygen concentration and Fe^{2+} oxidation;
(b) increasing the pH to 7.5 or higher to promote the Fe^{2+} oxidation rate;
(c) introducing an alternative oxidant such as chlorine that may be produced by oxidization of the chloride ions present in water/wastewater on the iron anode or in an additional electrolysis cell, for example using a Ti/RuO_2 anode and a Ti cathode [48]. Thereafter, ferrous oxidation takes place in the bulk solution, as shown below:

$$Cl_2 + H_2O \rightarrow ClOH + Cl^- + H^+ \tag{24}$$

$$2Fe^{2+} + 2HOCl \rightarrow 2Fe^{3+} + 2OH^- + Cl_2 \tag{25}$$
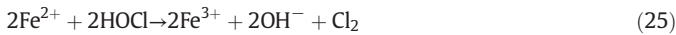
Taking into account the electric current consumed by chloride ions oxidation, this process is not efficient unless the water/wastewater to treat contains above 600 mg Cl^-/L.

(d) increasing the residence time to achieve complete Fe^{2+} oxidation.

Iron presents also two additional advantages over aluminum: iron is nontoxic thus it can be used for potable water, even though Moroccan guideline is 200 ppb for aesthetic and organoleptic reasons, which is exactly the same value as for aluminum. The second one is the lower price of iron, about 0.5–0.8 US$/kg, while aluminum cost lies between 1.5 and 3 US$/kg.

3. Key parameters influencing the EC process

The parameters affecting EC effectiveness are related to the operating conditions such as current or voltage and operation time, to water/wastewater features such as pH, alkalinity and conductivity and to the geometry of the EC reactor and the EC electrodes (electrode surface, electrode spacing).

3.1. Effect of current

Current I is a key parameter of EC. EC is often designed as a function of current density i defined as the ratio of current over electrode surface area S. The continuity equation imposes current conservation between the anode and the cathode, current density may differ between electrodes where

$$I = i_A \cdot S_A = i_C \cdot S_C \tag{26}$$

Current density determines the coagulant dosage at the anode and the hydrogen gas (H_2) evolution at the cathode governed by Faraday's law. The bubble density affects the system hydrodynamics, which in turn influences mass transfer between pollutants, coagulant and gas micro-bubbles, and finally dictates collision rate of coagulated particles that results in flocs formation [49]. Current density affects as well hydrolyzed metal species through pH evolution during EC process as a function of water alkalinity. The current appears, therefore, to create a dynamic physical/chemical environment that governs directly the coagulation/flocculation mechanism [33,50] and favors the electromigration of ions and charged colloids [51].

Cell voltage is correlated as a function of equilibrium potential, anode and cathode overpotential as postulated by Eq. (35). Electric energy consumption can then be deduced as a function of operation time t using:

$$P = \int_0^t U.I.dt \tag{27}$$

As electric energy required for the EC process is linked to the electric current and potential as shown in Eq. (27), EC can be driven either under the galvanostatic or potentiostatic mode. For the galvanostatic mode, EC process is carried out by controlling and/or varying the current applied through electrodes while for the potentiostatic mode, it is the applied cell voltage that is controlled and/or varied as a function of amount of coagulant desired to be released in EC reactor. The potentiostatic mode is rarely used for EC [52] and often used for other electrochemical methods such as electro-oxidation and electro-reduction when sacrificial electrodes are not used [53,54].

However, very high current values may negatively affect the EC efficiency. For instance, secondary reactions may occur chiefly, and overdosing can reverse the charge of the colloids and redisperse them
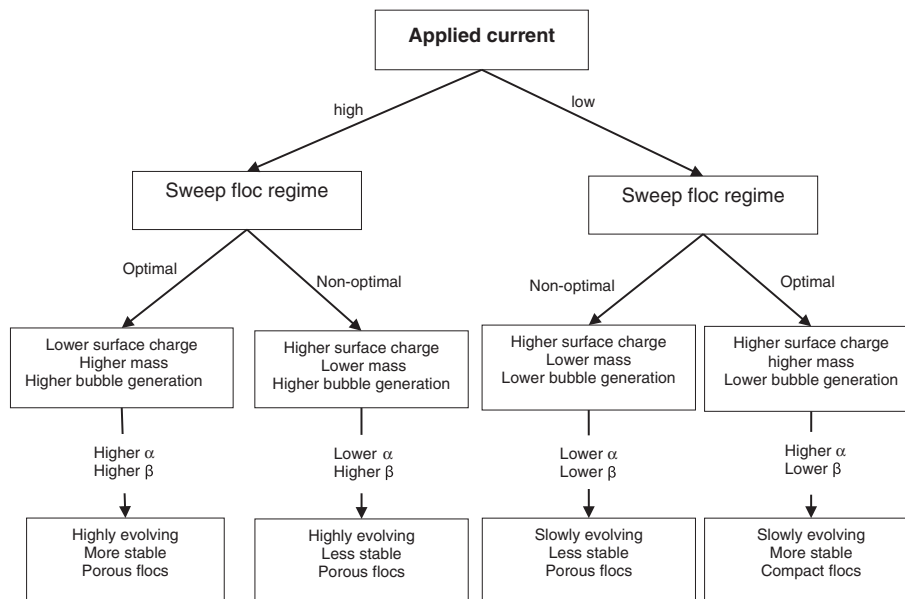
Fig. 5. Conceptual model predicting floc evolution rate and structure with α as collision efficiency and β as collision frequency [33].

leading thereby to a decrease of the coagulant efficiency and to a reduction of the electrode lifetime. For instance, in their work, after finding that size and structure evolution of flocs in EC of suspended colloid (kaolin) depend strongly on the current, Harif and Adin [33] suggested a model that describes also how applied electric current governs the rate, the structure and the features of flocs formed, their collision efficiency α and frequency β in the EC process (Fig. 5).

The values of the current density range may widely vary according to the features and the amount of pollutants to be removed from water/wastewater, for instance from 0.01 A·m^{-2} [55] to 880 A·m^{-2} [56]. Optimum current density should be determined considering other operating parameters. To operate the EC system for a long period without maintenance, current density is suggested to be between 20 and 25 A·m^{-2} [39]. High current also increases voltage and ohmic drop between anode and cathode; ohmic drop or IR drop results from the ohmic resistance of the electrolyte R, which can be expressed as follows:

$$R = \frac{d}{S} \frac{1}{k} \qquad (28)$$

where d denotes the inter-electrode distance and k the water conductivity. Indeed, when i increases, and U tends to the IR drop term RI deduced from Eq. (28), which means that electric power varies as RI^2. Consequently, power input can be reduced by decreasing the distance between the electrodes and increasing the electrode surface area and the water/wastewater conductivity [32]. Using current reversal (switching anode and cathode electrically) is useful to reduce maintenance cost, but its effect on pollution removal is not ascertained up to now.

3.2. Effect of water pH and alkalinity

pH is another key factor influencing the performance of EC, especially the coagulation mechanism because it governs the hydrolyzed metal species generated in reactive media and influences the prevailing mechanisms of EC [43]. A study of Al and Fe speciation resulting from hydrolysis of their corresponding cations governed by thermodynamic equilibrium is primordial to unravel how pH contributes to dictate the EC mechanisms, as already discussed in Section 2. Adsorption and coagulation particularly depend on pH. The superficial charge of the Al or Fe precipitates can be explained by the adsorption of the charged soluble monomeric species on their respective hydroxide precipitates [42]. Taking into account their superficial charge, the behavior between the pH-dependent coagulant species and their neighboring pollutants may be deduced from electrostatic interactions. A detailed analysis considering these mechanisms (double layer compression, neutralization and sweep flocculation) has been reported by Jiménez et al. [42] for Al and Fe-EC so as to maximize the abatement of different pollutants as a function of the prevailing hydrolyzed metal species. The importance of pH on EC performance can be equally underscored by the thermodynamics associated with electrochemistry as defined by the Nernst equation. This latter allows depicting E-pH diagram of an appropriate electrode material which, once superimposed on E-pH diagram of water leads to a diagram well-known as Pourbaix diagram that points out the regions of thermodynamically stable metal species in aqueous environment namely immunity, passivation and corrosion, which permits to predict the corresponding electrode stability and its dissolution behavior in water by defining the aqueous stable species in a given domain of electrochemical potential and pH.

Zongo [51] studied the Al and Fe speciation with the aim to establish the predominance diagrams of corresponding hydroxides and to assess a part of insoluble hydroxides as a function of pH considering only monomeric species. For Al electrode, it has been found that the amount of insoluble aluminum hydroxide increases sharply with increasing pH from 4.5 to 7 to the detriment of aluminum hydroxide ions and the reverse is true for a pH from 7 to 10, while amorphous metal hydroxide is

absent above the latter pH value . For Fe electrode, the quantity of insoluble iron hydroxide drastically increases with pH ranging from 4 to 7. At this latter pH value, iron hydroxide ions are absent on the predominance diagram. These predominance diagrams were obtained from the theoretical calculation based on equilibrium constants and pH for a concentration of 10^{-2} M for both electrode metals.

It is worth noting that effluent pH after EC treatment would increase for acidic influent but can decrease for alkaline effluent, which is due to the buffering effect of EC [57]. The increase of pH in acidic medium is due to hydrogen evolution at the cathode while the decrease of pH is due firstly to the formation of hydroxide precipitates that release H^+ cations at the anode vicinity and the secondary reactions such as water oxidation and chlorine production and its hydrolysis. This highlights the buffering effect of EC that acts in addition to that of water alkalinity. This effect is particularly high with Al electrodes because of the formation of aluminate anions at high pH [9].

The bicarbonate alkalinity has been reported to improve slightly the pollutants removal efficiency [58] and in addition it allows to remove the hardness by precipitation of $CaCO_3$ thanks to the hydroxyl anions produced by water reduction at the cathode vicinity [59].

3.3. Effect of cell geometry and electrodes design

The EC device is mainly made of electrodes and enclosure. The electrodes are arranged in an enclosure that is a non-conductive tank in which the treatment of water/wastewater takes place.

3.3.1. Electrodes arrangement

EC process can be affected by electrode system through electrodes arrangement and inter-electrode distance. Electrodes arrangement can
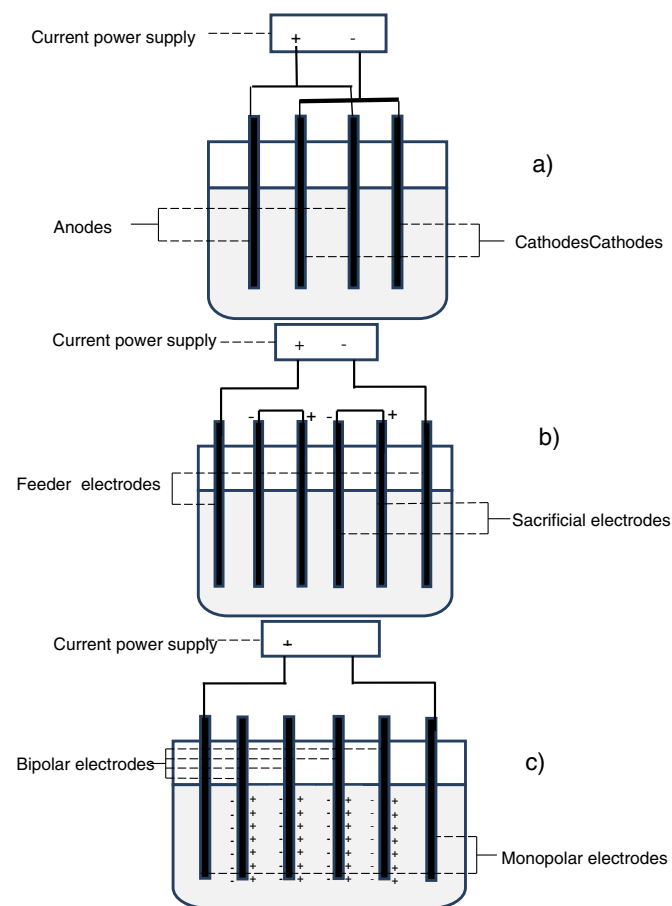
Fig. 6. Monopolar electrode a) in parallel connections b) in series connections; c) bipolar electrode in series connections.

either be simply composed of an anode and a cathode or be composed of many anodes and cathodes complexly settled in EC cell. The complex electrodes arrangement can be classified in monopolar and bipolar electrodes.

- Monopolar electrodes in parallel connection (MP-P) are described in Fig. 6a. It corresponds to an electrode arrangement that consists of cathodes and anodes placed alternatively at the same anodic or cathodic potential, respectively. Each pair of cathode/anode corresponds to a small electrolytic cell in which the voltage is the same. The reactor consists, therefore, of electrolytic cells in parallel. Consequently, the current of each electrolytic cell is additive.
- Monopolar electrodes in series connections (MP-S) are described in Fig. 6b. Each pair of internal sacrificial electrodes is internally connected with each other, and has no interconnections with the two outer electrodes. In this case, the electric current passing through all the electrodes is the same, whereas the global voltage is the sum of voltage in each individual electrolytic cell.
- Bipolar electrode in series connections (BP-S) comprises two outer electrodes connected to electric power supply and the sacrificial electrodes placed between the two outer electrodes (Fig. 6c). Outer electrodes are monopolar and the inner ones are bipolar. The bipolar electrodes are not interconnected and each of their sides acts simultaneously as an anode and a cathode. This means that opposite sides of each bipolar electrode are oppositely charged, the anodic dissolution takes place on the positive side while the negative side is prone to cathodic reactions [5].

Overall, monopolar electrodes require a low voltage and a higher current contrary to the bipolar electrodes that operate under a high voltage and a lower current. It is so difficult to conclude which electrodes arrangement is better than the other considering only EC yield given that it has been proved that equally BP-S could display a high EC efficiency [60,61]. Taking into account the ratio effectiveness-cost, monopolar electrodes may be deemed interesting because in many cases this electrodes arrangement offers a high pollutant removal with a lower energy consumption [62,63], knowing that bipolar electrode always consumes a high energy [64–66]. This last mode which is easy to handle, needs less maintenance cost during operation, thus the impact of maintenance cost on overall operation cost should equally be considered to choose an appropriate electrode mode [7].

Besides the popular rectangular electrodes, there are other geometrical shapes such as circular, cylindrical. Electrodes can be settled either vertically or horizontally in EC cell [30]. Despite being rarely used, horizontal electrodes in EC batch reactor may have a higher mixing efficiency [67].

3.3.2. Effect of inter-electrode distance

The IR-drop increases as the distance between electrodes increases. Thus, energy consumption decreases with decreasing the gap between electrodes (Eqs. (27) and (28)). As the distance between electrodes becomes lower, more electrochemically generated gas bubbles bring about turbulent hydrodynamics, thereby leading to a high mass transfer as well as to a high reaction rate between the coagulant species and pollutants [68]. In addition, inter-electrode gap defines the residence time between the anode and the cathode for a continuous system and the time of treatment for a batch reactor for reaching a desirable EC efficiency. For a complex electrode arrangement, Inter-electrode distance determines also the number of electrodes to place in electrocoagulation cell, once its volume is defined [69].

3.3.3. EC reactor design

EC reactor design is of great importance since it affects the overall performances of the EC process through its influence on the operating parameters namely, flow regime, flocs formation, removal yield and flotation/settling characteristics [38]. EC reactors have been designed following some key criteria, chiefly the operating mode and the goals to be reached. EC reactor design can be classified on the basis of three major distinctions according to literature survey [4,39]. The first one is whether a reactor is configured as a batch or a continuous system, i.e. the feed mode. For a continuous system, reactors are continuously fed in water/wastewater and operate, while the operation is carried out with a fixed wastewater volume per treatment cycle in a batch process [4]. The second distinction is the method used to separate the aggregated pollutants, as discussed in Section 2.1 and in illustrated Fig. 4. The last one is the design of the electrodes geometry that defines the current distribution in the cell: typical EC cells have been reviewed by Mollah et al. [32] and have not significantly change in the last decade. In practice, rectangular cells still dominate, as planar rectangular electrodes can be used, and the most common design in typical applications is the open vertical-plate cell, usually followed by a settler (Fig. 7). This means that it is open at the top, which avoids submerged contacts and make maintenance easier; vertical anodes and cathodes are equally spaced in parallel; any vertical/horizontal length ratio can be used, which makes scale-up easy, but maintenance is facilitated by values lower than 2. If current reversal is applied, the symmetry of the anode-cathode electrodes reduces maintenance, in particular in comparison to cylindrical EC cells. Described as the most versatile design in terms of flow rate, mixing is usually the main weakness of this cell geometry (Fig. 7b).

Alongside electrodes arrangement and electrodes spacing, EC reactor design affects EC through the reactor working volume that intervenes to define electrode area/volume ratio (A/V) and through EC geometry. Electrode A/V ratio is the only key scale-up parameter in plant design that allows developing EC full-scale equipment from laboratory experiments keeping the same inter-electrode distance when using electrode plates. The typical range of electrode A/V ratio varies between 15 m^2/m^3 and 45 m^2/m^3. An increase of the A/V ratio results in a decrease of both treatment time and the optimum current density [40]. When the electrode area is high enough, the major parameter is the current concentration I/V. This parameter combines the current density and the electrode area/volume ratio and allows defining the concentration of coagulants released in water at a given treatment time using Eq. (29) under batch conditions. Under continuous system, the reactor volume allows defining the residence time for a considered flow rate of water/wastewater and thus the released coagulant quantity can be deduced.

$$C = \frac{M}{ZF}\left(\frac{I}{V}\right) \cdot t \tag{29}$$

where C and V are the theoretical concentration of metallic cations (g/m^3) and the working volume of the EC device (m^3), respectively.

The usual reactor geometry, such as cylindrical, cubic and rectangular parallelepiped, has a slight effect on EC performance, except from a non-conventional shaped EC reactor known as an electrochemically-driven airlift reactor. Essadki et al. [72] studied the decolorization of textile dye wastewater by EC/electroflotation in an external-loop airlift reactor, usually used to carry out chemical and biochemical oxidations. The use of optimal current density and electrode position allowed removing 80% COD (chemical oxygen demand) and color from the textile dye wastewater. This highlights the key role that can be played by the EC reactor geometry in terms of hydrodynamic and mixing properties [72].

3.4. Effect of water conductivity

The current density efficiency depends strongly on conductivity and ionic strength of water/wastewater. The current density efficiency increases with increasing electrolytic conductivity due to the decrease of ohmic resistance of water/wastewater. Conductivity also decreases the
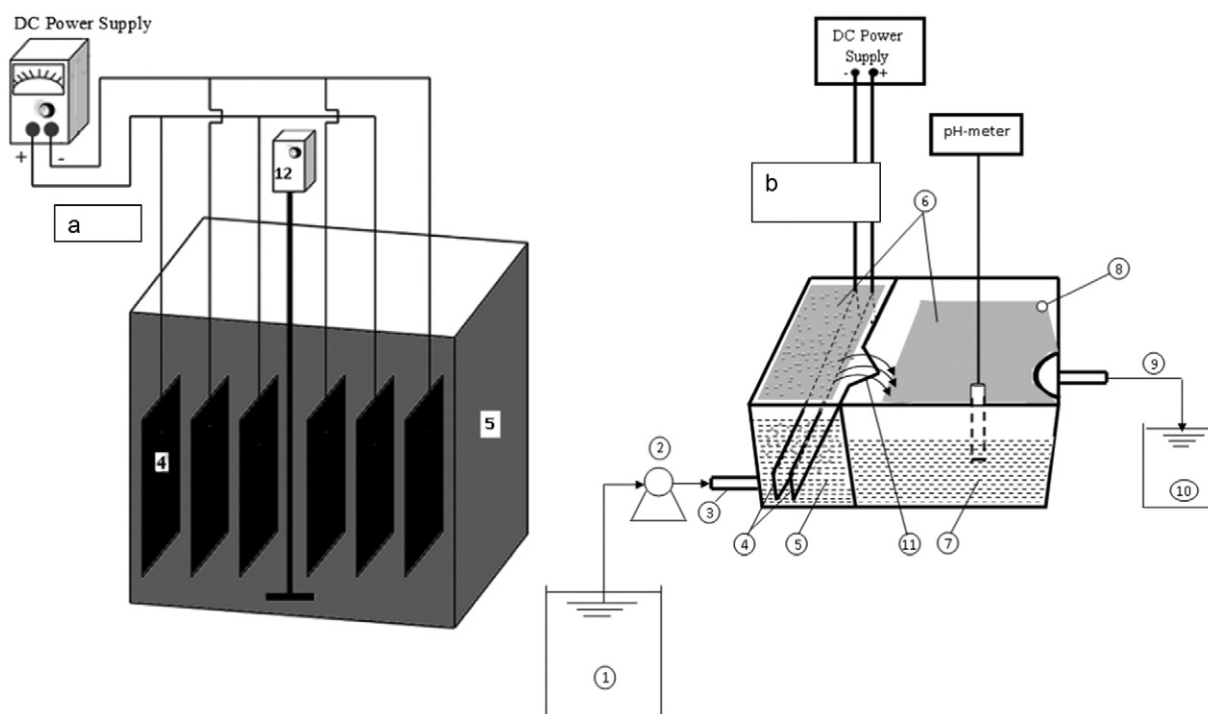
Fig. 7. Experimental setup of a) batch EC cell [70] b) continuous EC cell [71] (1: wastewater tank; 2: peristaltic pump; 3: effluent input to the first compartment; 4: electrodes; 4: EC cell / first compartment treatment; 6: sludge; 7: second compartment treatment; 8: sludge evacuation; 9: treated effluent evacuation; 10: treated water tank; 11: outfall; 12: mechanical stirrer).

treatment time required to reach a given removal yield [74]. Consequently, the energy consumption (UI) is reduced. NaCl is frequently used to increase the electrolytic conductivity. Chloride anions take part as well in the reduction of the adverse effects of other anions to avoid the precipitation of calcium carbonate in hard water that could form an insulating layer on the surface of the electrodes [57]. For very high current density, chloride anions can also be oxidized to active chlorine forms, such as hypochlorite anions, that can oxidize organic compounds [7] and ferrous ions [48] or contribute to water/wastewater disinfection. In order to ensure a normal operation of EC in wastewater treatment, it is recommended that 20% of the anions present should be Cl^- [39].

However, there are the constraints imposed on conductivity increase in wastewater treatment and particularly in potable water treatment. For wastewater treatment, besides a secondary pollution that could be produced by an increase of conductivity, there are the norms to be respected depending on whether the treated wastewater is devoted either to the reuse or to be flowed out in ecosystem. Conductivity increase during the treatment of drinking water by EC is highly limited in accordance with the standard norms that define the maximum chloride concentration in industrial effluents at 250 mg/L [73].

4. EC modeling

The literature review demonstrated the relative lack of systematic approach of EC reactor design and scale-up. The necessary improvements in EC cell performances and operation demand better design, materials, and optimization. These require a deep understanding of the interactions between many processes involved in EC, including electrochemical mechanisms, coagulation, flotation, and settling [32]. EC modeling is significantly helpful to improve the design and reduce both equipments and operating costs. It can quickly provide us robust and accurate solutions to EC problems, and thus enable us to predict EC cell performances under a wide range of operating conditions.

This section reviews EC models already reported and discussed in the literature and that can help to gain more insights in EC reactors design. There are two main classes of EC modeling: statistical modeling and modeling based on knowledge. Statistical modeling generally aims at seeking optimum operating conditions in which EC efficiency will be improved. EC being a complex process, modeling based on knowledge encompasses some models that consider EC as one process and some others that are used to describe a given physical or chemical phenomenon occurring during the process. Special attention is also devoted to computational fluid dynamics (CFD) modeling, where computational techniques have been applied to study fluid flow and current density inside EC reactors and predict complex inherent phenomena, especially in case where an experimental approach is restricted by technical constraints.

4.1. Statistical modeling

Considering many physical/chemical phenomena involved in EC, the pollutants removal efficiency complexly depends on the single and combined effects of the main process variables (factors). To date, in most studies on water/wastewater treatment by EC, optimization has been performed by varying a single factor while keeping all other factors fixed at a specific set of conditions. This habitual way for optimization of EC process requires many experimental runs and results in poor optimization, such as underestimation or overestimation of the effect of the process parameters on EC performances due to disregarding the interactions among those variables [75].

To solve this issue, response surface methodology (RSM) has been used as a tool in several works to display the effects of major process parameters and their interactions. RSM has many forms namely the full or partial factorial design (FD) [76–77], central composite design (CCD) [78–83], D-optimal design (DOP) [75], and Box-Behnken design (BBD) [84–87], among others. FD is used to determine the principal effects of independent variables and their interactions while CCD, DOP and BBD

are used to estimate the optimum operating conditions and to generate the empirical model represented by a second-order polynomial regression model given below:

$$Y = b_0 + \sum_{i=1}^{k} b_i X_i + \sum_{i=1}^{k} b_{ii} X_i^2 + \sum_{j=1}^{k} \sum_{i=1}^{k} b_{ij} X_i X_j \qquad (30)$$

where the X_i and X_j terms are the factors that influence the predicted response Y, b_0 is the average of the experimental response, b_i, b_{ii} and b_{ij} are the regression coefficients for linear, quadratic and interaction terms, respectively.

The determination of the optimal operating conditions should consist of seeking the ceiling and/or the bottom of the depicted response surface of process performance criterion according that this latter is to be maximized or minimized. The performance of EC process may be appraised by the efficiency removal of one or more of the parameters such as TOC (total organic carbon), COD, TDS (total dissolved solids), turbidity and specific pollutant. Several responses can be combined in a desirability function for multiple response optimization, including process costs. Therefore, optimization of EC using RSM will be carried out by maximizing the indicators of process performances while minimizing adequately the parameters related to the operating costs. According to the literature survey, RSM as a statistical experiment design turned out to be a powerful tool to effectively optimize the operating conditions, despite EC complexity, and generates second-order polynomials that represent well the quantitative relationship between responses (EC performance) and the critical process variables [78–89]. Fig. 8 summarizes the main factors that affect EC process; their interactions underline the vectors through which EC performances could be affected.

4.2. Modeling based on knowledge

4.2.1. Phenomenological models

EC kinetics has been studied in many works to model and to simulate EC process as well as designing EC system using classical kinetic law (Eq. (31)). Mameri et al. [40] were among the first researchers to attempt to model EC kinetics of the abatement of fluoride anions. In their works, kinetics of defluoridation was found to follow an exponential law with time, so that it turned out to be first-order with respect to fluoride concentration. Equally, the removal of some pollutants such as nitrates [24,90] and heavy metals by EC turned out to follow a n-order kinetic model [91,92].

$$\frac{dC}{dt} = KC^n \qquad (31)$$

where C, K and n are the initial concentration of the pollutant, the reaction rate constant and the order of reaction.

Upon the key findings of recent works, the kinetic law of the defluoridation by EC process should be a pseudo-first-order reaction since the kinetic constant K was found to be dependent on initial fluoride concentration [93,94]. These authors attempted to model the fluoride removal by expressing the kinetic rate constant K using an empirical model that fits the experimental data based on a first-order kinetics (Eqs. (33 and 34)) and the time necessary t_N to reach a targeted fluoride concentration was deduced using Eq. (32).

$$t_N = \frac{1}{K} \ln\left(\frac{C_0}{C_t}\right) \qquad (32)$$

$$K = 10^{-5}\left(5.9\left(\frac{I}{V}\right) - 37.1 C_0 - 82.1 d + 2746.4\right) \qquad (33)$$

$$K = 10^{-3}\left(-1.68 i^2 + 36.4 i - 12.6\,\mathrm{pH} - 0.5 C_0^2 - 7.61 k + 250\right) \qquad (34)$$

where C_0 and C_t denote the initial and final concentration, k the conductivity, V the working volume and d the inter-electrode distance.

In the work of Essadki et al. [94], the defluoridation kinetics was studied in an external-loop airlift reactor. The similar critical variables in both empirical models were current concentration or current density and initial fluoride concentration. Kinetic constant in both equations increased with increasing electric current (current concentration or current density), contrary to the initial fluoride concentration. In some works on EC, kinetic law was defined by postulating a rate constant in Arrhenius form as for an ordinary chemical reaction to account for temperature dependence [95,96].

4.2.2. Modeling detailed mechanisms

4.2.2.1. Electrochemical phenomena:
Among the fundamental sciences on which EC is based, electrochemistry is the main one given that the electrochemical phenomena are the triggering core of the whole process. Electrochemistry should be considered as a complex science
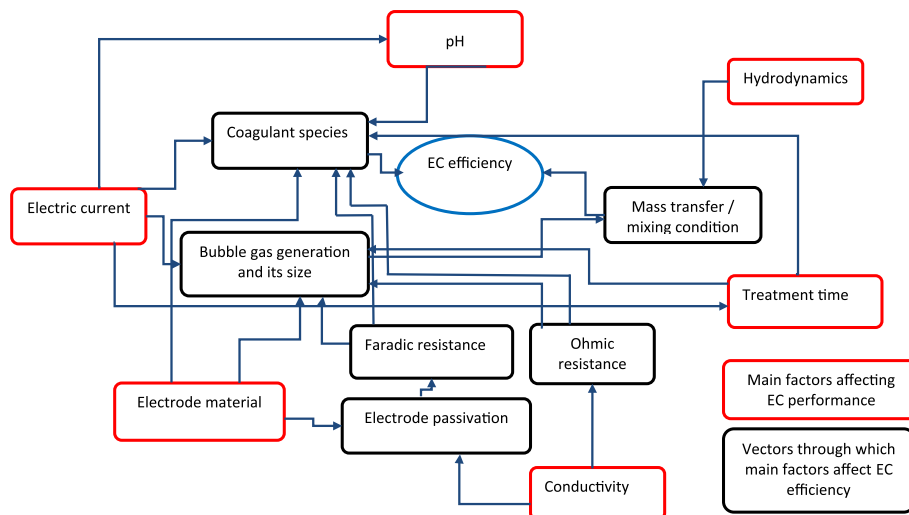

Fig. 8. Main factors that affect EC process.

accompanied by charge transport, electrochemical kinetics, knowledge of electrodes interface and thermodynamics.

Once there is a potential applied across electrodes, it results in an entropy creation that puts the system out of equilibrium. Applied potential must overcome the equilibrium potential difference, anode and cathode overpotential and ohmic potential drop of the solution as shown in Eq. (35) [97].

$$U = E_{eq} + \eta_{a,a} + \eta_{a,c} + \eta_{a,p} + |\eta_{c,a}| + |\eta_{c,c}| + |\eta_{c,p}| + \frac{d}{k}i \quad (35)$$

$\eta_{a,a}$, $\eta_{a,c}$ and $\eta_{a,p}$ are the anode activation overpotential, concentration overpotential and passivation overpotential, respectively. $\eta_{c,a}$, $\eta_{c,c}$ and $\eta_{c,p}$ are the cathode activation overpotential concentration overpotential and passivation overpotential, and the last term defines the IR drop of the solution, while E_{eq} is the equilibrium potential difference calculated between the anode and the cathode, respectively, using the Nernst equation with assumption of ideality given below:

$$E = -\frac{\Delta G^0}{ZF} + \frac{RT}{ZF} \sum \nu_i \ln\left(\frac{C_i}{C^\circ}\right) \quad (36)$$

where ΔG^0 denotes the standard Gibbs free energy, C the concentrations, T the temperature and R the ideal gas constant. Application of electric current is ensued by electrolytic reactions; thus, there is a charge exchange on electrode interface. The electrochemical reaction rate is defined below:

$$Ox + Z \cdot e^- \leftrightarrow Red \quad (37)$$

$$r = \frac{d\xi}{Sdt} = \frac{dq}{ZSFdt} = \frac{i}{ZF} \quad (38)$$

Z is the number of electrons involved in the reaction, S the electrode surface, ξ the degree of advancement of the reaction and q the charge. Assuming that the electrochemical reaction rate follows a first-order mechanism, the overall current density is postulated as follows:

$$i = i_a - i_c = ZF(k_{oxy}C_{red} - k_{red}C_{oxy}) \quad (39)$$

After defining the constant rates of oxidation and reduction on the basis of the activated complex theory and in the case the reaction rate is controlled only by electrical charge transfer on electrode interface, Eq. (39) leads to Butler-Volmer equation:

$$i = i_0 \left[\exp\left(\frac{(1-\alpha)ZF\eta}{RT}\right) - \exp\left(\frac{-\alpha ZF\eta}{RT}\right) \right] \quad (40)$$

where i_0 is the exchange current density and α a transfer coefficient

• For the low values of overpotential, η that are close to equilibrium potential difference, the current density can be written as:

$$i = i_0 \frac{ZF\eta}{RT} \quad (41)$$

• For the high values of overpotential η, the current density can be written as
  - Cathodic current density:

$$i = i_0 \cdot \exp\left(\frac{(1-\alpha)ZF\eta}{RT}\right) \quad (42)$$

  - Anodic current density:

$$i = -i_0 \exp\left(\frac{-\alpha ZF\eta}{RT}\right) \quad (43)$$

Positive or negative overpotential can be written in a logarithmic form, known as Tafel equation:

$$\eta = \alpha + \beta \ln i \quad (44)$$

These above (anodic and cathodic) constants of the Tafel equation are determined on the basis of the curve of overpotential plotted as a function of logarithm of current density [14,98]. Thereafter, the potential in Eq. (35) can be described in detail as follows:

$$U = E_{eq} + \frac{d}{k}i + (\beta_a + \beta_c) \cdot \ln i + \eta_{a,c} + |\eta_{c,c}| + K \frac{i^n}{k^m} \quad (45)$$

where the last term corresponds to the global passivation overpotential. Cell potential U required by non-passivated and passivated electrodes when diffusion in the mass transfer boundary layer of the electrodes is not limiting can be modeled in the simple forms reported below [97]:

$$U = K_0 + \frac{d}{k}i + K_1 \ln i \quad (46)$$

$$U = K_0 + \frac{d}{k}i + K_1 \ln i + \frac{K_2}{k^m} i^n \quad (47)$$

where K_0, K_1 and K_2 are the constants to be determined.

Once a large overpotential is applied, mass transfer, i.e. concentration overpotential, becomes the limiting step that determines the reaction rate. The latter is reliant on three main phenomena namely diffusion, electronic migration and convection. Mass transfer including those three phenomena can be calculated by Nernst-Plank equation that will be detailed later.

4.2.2.2. Adsorption and VOK model: Typical adsorption isotherm and adsorption kinetics models have been widely used to better understand the mechanisms involved in EC and for modeling purpose. Since the amount of coagulant generated can be estimated for a given time using Faraday's law, pollution abatement can be modeled from the adsorption phenomenon [99]. The most common adsorption isotherms used for EC modeling with the assumption of thermodynamic control are namely, the Langmuir and Freundlich isotherms and the Langmuir–Freundlich model that combines the two previous ones. The Langmuir isotherm assumes a monolayer deposition of the adsorbate on a homogenous adsorbent surface, while the Freundlich isotherm describes reversible adsorption that may be accompanied by multilayer formation [100]. The various isotherm models are given below:

$$\text{Langmuir isotherm} : q_e = q_{max} \frac{K_L C_e}{1 + K_L C_e} \quad (48)$$

$$\text{Freundlich isotherm} : q_e = K_F C_e^{1/p} \quad (49)$$

$$\text{Langmuir-Freundlich} : q_e = q_{max} \frac{K_{LF} C_e^n}{1 + K_{LF} C_e^n} \quad (50)$$

where q_e is the amount of adsorbed molecules per amount of adsorbent at equilibrium, C_e is the equilibrium adsorbate concentration in water, q_{max} is the adsorption capacity of adsorbed molecules per amount of metal cations, K_L is the Langmuir constant, K_F and p are the Freundlich parameters and K_{LF} and n are the Langmuir-Freundlich parameters. The amount of removed adsorbate by adsorbent at equilibrium in a

batch system is estimated as shown below:

$$q_e = V \frac{C_0 - C_e}{m_{M(OH)_3}} M_{M(OH)_3} \qquad (51)$$

Alongside adsorption isotherms, there are adsorption kinetics models also used in EC process to predict the pollutant removal namely, the pseudo first-order and the pseudo-second-order kinetic models [101–104]. The pseudo-first-order adsorption kinetic model assumes that the rate of occupation of the adsorption sites is proportional to the number of unoccupied sites while the pseudo-second-order kinetic model describes the adsorption equilibrium. Their respective mathematical expressions are:

$$\frac{dq_t}{dt} = k_1(q_e - q_t) \qquad (52)$$

$$\frac{dq_t}{dt} = k_2(q_e - q_t)^2 \qquad (53)$$

where q_e and q_t are the amounts of adsorbate adsorbed on the adsorbent at equilibrium at any time t, respectively, and k_1 and k_2 are the rate constants. Other adsorption kinetic models, such as the Elovich and intraparticle diffusion model, have been used in EC process as well [104].

A new approach known as a variable-order-kinetic model (VOK) derived from adsorption isotherm models combined with Faraday's law was first introduced by Hu et al. [11]. A VOK model that has been used in the defluoridation, turned out to be efficient to estimate the required time for fluoride removal by EC using Al electrode [11,94]. VOK assumes that the defluoridation rate is related to the amount of Al^{3+} electrolytically generated. The latter is the rate-determining step of defluoridation, especially when EC operates under lower current density (under 200 A/m^2 [11]). Spontaneous hydrolysis of Al^{3+} leads to coagulant formation and the suitable adsorption isotherm serves to define the maximum adsorption capacity of a mole of $Al(OH)_3$. Thereafter, the kinetic law of fluoride removal can be expressed as follows:

$$-\frac{dC_t}{dt} = \phi_M q_e \frac{dM_{tot}}{dt} \qquad (54)$$

where ϕ_M is the efficiency of hydro-fluoro-aluminum formation, M_{tot} represents the total aluminum dosage liberated from the anode and its rate can be deduced from Faraday's law with ϕ as the current yield:

$$\frac{dM_{tot}}{dt} = \phi \frac{I}{Z \cdot F \cdot V} \qquad (55)$$

VOK model assumptions combined with various isotherms lead to the following equations:

• Langmuir isotherm:

$$-\frac{dC_t}{dt} = \phi_M . \phi \frac{I}{ZFV} q_{max} \frac{K_L C_e}{1 + K_L C_e} \qquad (56)$$

• Freundlich isotherm:

$$-\frac{dC_t}{dt} = \phi_M . \phi \frac{I}{ZFV} K_F C_e^{1/p} \qquad (57)$$

• Langmuir-Freundlich:

$$-\frac{dC_t}{dt} = \phi_M . \phi \frac{I}{ZFV} q_{max} \frac{K_{LF} C_e^{n,}}{1 + K_{LF} C_e^{n,}} \qquad (58)$$

Hu et al. [11] reported that a VOK model based on Langmuir isotherm was an appropriate kinetic model to represent defluoridation

rate with Al electrodes. Similarly, Essadki et al. [94] studied the defluoridation kinetics of drinking water treated by EC in stirred tank reactor where the fitting isotherm was Langmuir-Freundlich. The discrepancy with the results obtained by Hu et al. [11] was explained by the different operating conditions in terms of stirring conditions and electrode A/V ratio. Essadki et al. [94] used a A/V ratio extremely lower than the conventional range of A/V values in a large mechanically stirred reactor (20 L). The corresponding mathematical expressions of the retention time for the removal of a given residual fluoride concentration defined by VOK based on Langmuir isotherm [11] and on Langmuir-Freundlich isotherm [94], are:

$$t_N = \frac{ZFV}{\phi_M \phi I q_{max}} (C_o - C_e) + \frac{1}{k} \ln\left(\frac{C_o}{C_e}\right) \qquad (59)$$

$$t_N = \frac{ZFV}{\phi_M \phi I q_{max}} \left[(C_o - C_e) + \frac{1}{K_{KL}(1-n)} \ln\left(C_o^{(1-n)} - C_e^{(1-n)}\right) \right] \qquad (60)$$

Essadki et al. [94] outlined where the difference comes if EC followed either the VOK model coupled with the adsorption isotherm or the pseudo-order kinetics after performing the defluoridation of drinking water in stirred tank reactor and in external-loop airlift reactor. In view of their results in the stirred tank reactor, the authors stated that when mixing is enhanced, an increase in mass transfer rate results, hence the limiting step is the adsorption capacity of the adsorbent. Thus, the VOK model associated with isotherms could be used to model EC process. The pseudo-order empirical kinetic which fitted the experimental data in the external-loop airlift reactor, could be employed elsewhere, when poor mixing conditions prevailed, the limiting step being mass transfer.

4.2.2.3. Flocculation modeling: Flocculation is a process whereby two or more colliding destabilized particles adhere together and form a floc. Mechanisms occurring during flocculation can be split into two steps: transport leading to the collision and attachment. The former is induced by (a) Brownian motion of the particles (perikinetic flocculation), (b) fluid motion (orthokinetic flocculation) and (c) differential settling velocities due to gravity (differential sedimentation). Attachment results from the interparticle forces. The rate of successful collision between particle I and j can be expressed as follows [105]:

$$r_{flocculation} = \alpha \beta(i,j) n_i n_j \qquad (61)$$

where α is the collision efficiency, $\beta(i,j)$ is the collision frequency between particles of size i and j, and n_i and n_j are the particles concentrations of particles of size i and j respectively.

The classical equation proposed by Smoluchowski has formed the core of subsequent research into flocculation modeling [105]. The overall equation defines the rate of change in the number concentration of particles of size k:

$$\frac{dn_k}{dt} = \frac{1}{2} \sum_{i+j=k} \beta(i,j) \cdot n_i \cdot n_j - \sum_{i=1}^{\infty} \beta(i,k) \cdot n_i \cdot n_k \qquad (62)$$

$\beta(i,j)$ and $\beta(i,k)$ are the collision frequency between the particles of size i and j, and between the particles of size I and k, respectively. n_i, n_j and n_k are the particle concentrations for particles of size i, j and k, respectively. The first summation defines the increase of particles of size k by flocculation, whereas the second one defines the loss of particles of the same size.

Although Smoluchowski approach made the simplifying assumptions to render his equation applicable to the flocculation process, the successful applications of that equation are limited to the idealized systems. Thomas et al. [105] concluded that the application of the flocculation modeling to real system requires renewed efforts in experimental work, based on advanced techniques. The fractal theory that allows

quantifying a disordered system, has been used to characterize flocculation kinetics by describing the fractal dimension associated with aggregate growth and structural properties of aggregate. Fractal aggregates are self-similar and the concept of the fractal theory based on power law behavior can be expressed as follows [106,107]:

$$M \propto r^{D_f} \tag{63}$$

where M is the mass, r the radius of a particular aggregate and D_f the mass fractal dimension. The latter can take values that range from 1 to 3. The minimum value corresponds to a line of particles and the maximum corresponds to a solid sphere of particles. The fractal dimension measurement has been performed using scattering, image analysis and sedimentation velocity [106]. Flocculation may occur following particle-cluster aggregation and/or cluster-cluster aggregation [108]. Considering cluster-cluster and irreversible perikinetic aggregation, two limiting regimes have been identified, namely diffusion-limited cluster aggregation (DLCD) and reaction-limited cluster aggregation (RLCD) [106]. DLCD takes places once there are little repulsive forces between particles and the particles stick to each other, thereby resulting in the formation of tenuous structure. The limiting step is the time required for the particles or clusters to approach each other. RLCD occurs when there are substantial repulsive force between particles; thus, the successful collision requires many collision frequencies to form a stable floc [30]. On the basis of computer simulations on cluster-cluster aggregation, two limits have been pointed out: a low mass fractal dimension ($D_f < 1.8$) that corresponds to DLCD and a high mass fractal dimension ($D_f > 2.1$) that corresponds to RLCD [106].

Flocculation modeling has not been applied in EC, apart in Ofir's work where the overall kinetic model of flocculation that embeds the floc break-up rate in turbulent mixing developed by Argaman and Kaufman was used [109]. However, the fractal dimension has been increasingly used in EC process to study the floc growth, the geometrical characteristics of the flocs and to deduce which aggregation regime governs the flocculation [6,30,33].

4.2.2.4. Flotation and settling: The aggregated flocs resulting from the water/wastewater treatment by EC may be removed by diverse physical methods, as described in Fig. 4. Electroflotation occurs due to buoyancy forces and settling due to gravity. Electroflotation depends on current density, hydrogen micro-bubbles size (20–50 μm) and particle collection efficiency by the micro-bubbles [4]. Although the current density dictates an appropriate pollutant removal path, especially in batch systems, it is impossible to completely avoid either settling or electroflotation in favor of the other mechanisms, whatever the current density that may be used.

Holt et al. [4] pointed out why the dissolved air flotation models described in the literature comprised of the population model balance and the white water collision model could not be fitly applicable to electroflotation. These consider two distinct zones, the reaction zone that favors the contact between the gas bubbles and the particles and the separation zone where the particles or aggregated pollutants attached on bubbles and float to the surface, while in batch EC reactor, the reaction zone and separation zone are one. These authors tried to adopt the white water collision model to the EC process where a hydrogen bubble was considered as a collector of particles/flocs and this model was extended from single bubble collector to a swarm of bubbles. The total single collector bubble efficiency was considered as the sum of a combination of Brownian diffusion interception, interception of the particle by bubble, sedimentation of the particle onto the bubble and inertial driven contact [4].

In his study, Holt [6] proposed an EC model whose main aim was to highlight the pollutants removal paths that consider the competitive process between settling and flotation in pollutants removal. Assuming the removal of pollutant in the bulk solution (C_{poll}) follows first-order kinetics, the latter is defined as the resulting kinetics of electroflotation

and sedimentation where the balancing parameter is the electric current:

$$\text{Pollutant}(C_{poll}) \xrightarrow{k_1} \text{Surface}(C_{surface}) \tag{64}$$

$$\text{Pollutant}(C_{poll}) \xrightarrow{k_2} \text{Base}(C_{Base}) \tag{65}$$

$$r_{poll} = -\frac{dC_{poll}}{dt} = k_1 C_{poll} + k_2 C_{poll} = (k_1 + k_2)C_{poll} \tag{66}$$

where k_1 and k_2 are flotation rate constant and settling rate constant, respectively, determined from experimental runs.

Once the flocs/sludge become heavier than aqueous media, they are prone to settle at the terminal velocity and are consequently entrained to the bottom of EC reactor. The sludge settling velocity models found in the literature (Eqs. (67)–(72)) have been used to correlate this quantity to the sludge solids concentration in EC process [110]. For instance, third-order, fourth-order and Cho's models fitted the experimental data of the sludge settling velocity for the treatment of chemical mechanical polishing wastewater by EC [110] and the first three models were used to characterize settling of the sludge obtained from the treatment of textile wastewaters [111]. Although they have been used, these models are not really precise enough to correlate the sludge settling velocity in the EC process due to the presence of hydrogen bubbles that is not taken into consideration.

• Power:

$$V = k S_c^{-x} \tag{67}$$

• Exponential:

$$V = k \exp(-n S_v) \tag{68}$$

• Cho's exponential:

$$V = k \frac{\exp(-n S_c)}{S_c} \tag{69}$$

• Third order:

$$V = k \frac{(1-n S_c)^3}{S_c} \tag{70}$$

• Fourth order:

$$V = k \frac{(1-n S_c)^4}{S_c} \tag{71}$$

• Cho's complex exponential:

$$V = k \frac{(1-n_1 S_c)^4}{S_c} \frac{\exp(-n_2 S_c)}{S_c} \tag{72}$$

where V is the sludge settling velocity, S_c the solid concentration, k, n, n_1 and n_2 are the model parameters that have to be determined experimentally.

4.2.2.5. Complexation: Complexation model is a recent phenomenological model describing adsorption equilibrium that results from

complexation of suspended matter by iron or aluminum hydroxides for COD abatement. EC proceeds by complexation of suspensions by metal species that can be characterized by chemical equilibrium postulated below [112]:

$$M + nS \rightarrow M{-}S \tag{73}$$
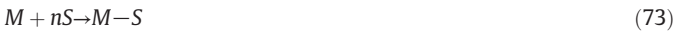
where n is the overall coefficient expressed in mg of dissolved metal over mg of oxygen (unit of the considered parameter). The overall equilibrium constant of this complexation reaction is expressed as:

$$K = \frac{[M{-}S]}{[M][S]_C} \tag{74}$$

$[M]$ is the concentration of free metal species, $[M-S]$ the concentration of the complexed form and $[S]_C$ the concentration of matter that can be complexed. The mass balance of suspended matter that can be treated is given by:

$$[S]_{c,t=0} = [S]_0 {-} [S]_f = [S]_c + \frac{[M{-}S]}{n} \tag{75}$$

with $[S]_0$ the initial concentration of suspended matter, and $[S]_f$ the concentration of suspended matter that cannot be treated by EC after addition of large excess of coagulant. Mass balance of metal species can be written as:

$$[M]_t = [M] + [M{-}S] \tag{76}$$

After replacement of $[M - S]$ and $[M]$ using Eqs. (75) and (76), Eq. (74) leads to the following equation:

$$[S]_c^2 + [S]_c \left(\left(\frac{[M]_t}{n} - [S]_{c,t=0} \right) + \frac{1}{K} \right) - \frac{[S]_{c,t=0}}{K} = 0 \tag{77}$$

At a given treatment time, the suspension concentration is given by the expression bellow:

$$[S]_c = [S]_f$$
$$+ \frac{-\left(\left(\frac{[M]_t}{n} - [S]_{c,t=0} \right) + \frac{1}{K} \right) + \sqrt{\left(\left(\frac{[M]_t}{n} - [S]_{c,t=0} \right) + \frac{1}{K} \right)^2 - 4\frac{[S]_{c,t=0}}{K}}}{2} \tag{78}$$

$$[S] = [S]_f + \frac{[S]_{c,t=0}}{1 + K\frac{[M]_t}{n}} \tag{79}$$

This empirical model was found to accurately fit experimental data [112,113]. In the case of a lower COD, Eq. (77) may be simplified in the first-order polynomial, Eq. (78) leads to Eq. (79) [113].

Merzouk et al. [114] developed two models, namely the overall model and the contribution model on the basis of a single-waste treatment model previously established within the framework of assessing the efficiency of EC treatment of two mixed effluent formed by addition of the red dye solution to the textile wastewater. For the treatment of mixed wastes, two different "species" S and T may be complexed by Al (III) species, as follows:

$$Al(III) + n_1 S \rightarrow AlS \tag{80}$$

$$Al(III) + n_2 T \rightarrow AlT \tag{81}$$

The first model called the "overall model" assumes that the EC treatment of mixed waste occurs regardless of the origin of the effluent. This model is represented by Eq. (82) based on the analogy of the above depicted Eqs. (73)–(78), and knowing X and Y (instead of $[S]_C$) may be the absorbance, the turbidity, the COD and the TOC of the red dye and the textile wastewater respectively.

$$Z = Z_f + \frac{-\left(\frac{[Al]_t}{n_3} - (Z_o - Z_f) + \frac{1}{K_3} \right) + \sqrt{\left(\frac{[Al]_t}{n_3} - (Z_o - Z_f) + \frac{1}{K_3} \right)^2 + \frac{4(Z_o - Z_f)}{K_3}}}{2} \tag{82}$$

where $Z_o = (X_o + Y_o)$, $Z = (X + Y)$, k_3 and n_3 are adsorption equilibrium parameters.

The second model, known as the "contribution model", is based on the separated contributions. The two "species" S and T are considered to adsorb on metal hydroxide independently, with parameters K_1 and n_1 and K_2 and n_2, respectively.

$$X = X_f + \frac{K_1(X_0 - X_f)}{n_1 + K_1[Al]} \tag{83}$$

$$Z = Z_f + \frac{K_2(Z_0 - Z_f)}{n_2 + K_2[Al]} \tag{84}$$

The two models fitted adequately the experimental data for turbidity and TOC, but the contribution model was found more reliable due to shortage of interactions of the two effluents in terms of turbidity and TOC in the mixed effluent. In contrast, the contribution model could not be applied to the absorbance and COD given that the absorbance measurements of the separate liquids were carried out at different wavelengths and the sum of COD of two effluents was higher than that of the mixed effluent COD.

It has been inferred from the treatment of mixed effluent considering turbidity and TOC that the treatment of several pollutants contained in wastewater from various effluents by EC could be considered the superimposition of the various treatments of single-species effluents, provided that the mixture of these effluents does not induce the destabilization of the suspensions formed by the mixed effluent or produce a chemical reaction in this medium.

4.3. Modeling by means of computational fluid dynamic (CFD)

Nowadays, as in many research areas, CFD simulations have an important part to play in understanding and improving EC reactors design for future applications. There are some studies on various aspects of flows through electrochemical cells [115–117]. CFD turns out to be helpful and attractive in understanding the hydrodynamic and residence time distribution to characterize the flow pattern and can be advantageously employed to predict the main local features of the process, like velocity profiles, the reaction rate distribution at the electrodes, the cell voltage, etc. In a recent work, CFD has been used to study the distribution of potential and current density since the latter determines the distribution of attack on electrode surface during its dissolution and can be useful in the EC reactor design for energy efficiency [115].

Simulations of the phenomena in an EC process involve the numerical solution of equations of motion (mass, momentum) and of energy, electric potential and current distribution in the flow geometry, together with other sets of equations related to the problem at hand (concentrations, turbulence…). In particular, the other set of equations are usually used to describe the transport mechanics, such as diffusion and migration in the presence of an electric field, and reactions of chemical species.

The flow pattern in EC cells may be either laminar or turbulent. In complex geometries, the velocity field includes a random turbulent component, which generates jet flows and turbulent eddies [118]. In many cases, turbulence models can be used to simulate accurately the flow pattern. The governing equations for an incompressible turbulent flow can be stated as follows. Mass balance in Cartesian coordinate

system is given by:

$$\frac{\partial \rho}{\partial t} + \rho \frac{\partial u_i}{\partial x_i} = 0 \tag{85}$$

where ρ is the fluid density and u is the mean-averaged velocity vector.

The momentum equation is usually described by the general RANS (Reynolds-Averaged Navier-Stokes) equation:

$$\frac{\partial(\rho u_i)}{\partial t} + \frac{\partial(\rho u_i u_j)}{\partial x_j} = -\frac{\partial p}{\partial x_i} + \frac{\partial}{\partial x_j}\left(\mu \frac{\partial u_i}{\partial x_j}\right) + \frac{\partial}{\partial x_j}\left(-\rho \overline{u_i' u_j'}\right) + \rho g_i \tag{86}$$

where u' is the fluctuating or turbulence velocity, p is the pressure and μ is the dynamic viscosity. The last modeled term is the turbulence stress $(-\rho \overline{u_i' u_j'})$. The simple model used by many authors is the standard k-ε model [115]. The governing equations for turbulent kinetic energy k and the energy dissipation rate ε can be inferred from reference [118].

The conservation of species and charge is given by:

$$\frac{\partial C_i}{\partial t} = -\nabla N_i + R_i \tag{87}$$

where C_i is the averaged concentration and N_i is the flux of chemical species due to convection, electromigration and diffusion and is expressed with the Nernst-Planck equation:

$$N_i = C_i u - Z_i u_{m,i} F C_i \nabla \phi - D_i \nabla C_i \tag{88}$$

here, Z_i is the charge number, u velocity, $u_{m,i}$ is mobility of species i, and D_i is the diffusion coefficient.

There are three types of distribution of current and potential. Primary current/potential distribution does not take into consideration the charge transfer on electrode due to the negligible overpotential and negligible concentration gradient. Secondary current/potential distribution considers the overpotential of activation whereby charge transfer takes place on electrode surface. Overpotential of concentration is neglected since the current density is still low in comparison to the limiting current defined by diffusional mass transfer in the mass transfer boundary layer of the electrodes. Tertiary current/potential distribution is obtained when there is a concentration gradient close to the electrodes due to an increase of current above the limiting current. There is thus a superimposition of overpotential of concentration on overpotential of activation [119].

In the absence of mass transfer limitation, the uniformity of the current distribution is a function of the Wagner dimensionless number:

$$W_a = \frac{K}{L}\frac{d\eta}{di} \tag{89}$$

$$\nabla^2 \Phi = 0 \tag{90}$$

$\frac{d\eta}{di}$ is the slope of anodic polarization ($\Omega \cdot m^2$), K the electrolyte conductivity ($S \cdot m^{-1}$) and L the characteristic length of the system (m).

Primary current distribution (Wa $\ll$ 1) depends only on system geometry and is calculated using the Laplace equation of the electric potential (Eq. (90)) where its integration provides the spatial distribution of potential when the boundary conditions are known [119]. Generally, an electrochemical cell is completely enclosed by at least an anode, a cathode and insulated walls on which (a) $\frac{d\phi}{d\eta} = 0$ and (b) potential or current are constant on the surface of the electrodes. In the bulk, the actual distribution of current is deduced from that of the potential by means of Ohm's law, as follows:

$$I = -K\nabla \Phi \tag{91}$$

The gradient of potential that is perpendicular to the electrode is used to estimate the current density on the electrodes [120].

For the secondary current distribution (Wa $\gg$ 1), the activation overpotential adds an equalizing effect on the current distribution, since the charge transfer resistance at the interface becomes large in comparison to the resistance of the solution. The calculation principle remains the same as for the primary distribution [119]. However, the boundary condition of the equation is no longer valid because of the potential jump at the interface that must be known. Tafel equation is usually applied on both electrodes. Tertiary current distribution accounts for ohmic effects, charge transfer effects in electrode kinetics, and the effects of concentration variations on the performance of the cell, in particular mass transfer boundary conditions.

The potential equations with corresponding boundary conditions are solved in order to find the electric potential and current density in the electrolyte. The Navier-Stokes equation (Eqs. (85) and (86)), mass conservation equations for each species (Eq. (88)) can be solved in the computational domain using some commercial software package like the finite-element COMSOL Multiphysics or the finite-volume ANSYS software package. As an illustration, Fig. 9b depicts the velocity field and secondary potential distribution inside an EC rector, while Fig. 9a displays the flow pattern inside the cell including different hydrodynamic phenomena like short-circuiting, recirculation and dead zones that can affects formation of flocks and aluminum concentration.

CFD was used successfully to describe the hydrodynamics and the complex flow pattern in the flow cell [116]. Several hydrodynamic phenomena were observed inside EC cells such as channeling, internal recirculation or dead zones. This complex behavior is inherent to cell geometry. CFD simulations and calculations of secondary- and tertiary-current distribution can be used to analyze the mass transfer in the electrolyte and reaction kinetics at the electrodes, and as a starting point to develop experimental-theoretical studies to improve the cell design, arrangement of electrodes as well as other modifications that increase their performance. CFD is theoretically able to address multiphase flows, e.g. those involving a dispersed solid and a dispersed gas phase, and even to account for particle and bubble size distributions through a population balance approach [121].

CFD presents, however, serious drawbacks and limitations. First, CFD requires expertise, in particular for mesh generation and critical analysis of the simulations. Simulations may be time-consuming, due to the complex coupling between the electrical field, species transport equations and Navier-Stokes equations, especially if tertiary current distribution is accounted for. In addition, recent studies on EC involving CFD use rough approximations on the physics of the process, neglecting the influence of hydrogen microbubbles and solid particles on the flow, because of the CPU and memory requirements of multiphase flow simulations.

4.4. Discussion

The past and recent approaches devoted to EC modeling have been summarized in details in this review. On the one hand, statistical modeling using RSM helps improve the effectiveness of EC by finding the optimum operating conditions, considering the possible interactions between different variables, but this methodology is obviously inadequate for scale-up purpose. On the other hand, modeling based on knowledge comprises more and more models that can be divided into those considering EC as a global process, and others that describe more or less precisely the various physical or chemical phenomena occurring aside, which requires a good knowledge of the mechanisms responsible for pollution removal. In EC, the electrochemical phenomena involved in the process have a vital role and run under the science of electrochemistry added to charge transport, electrochemical kinetics, knowledge of electrode interface and thermodynamics. Their description is compulsory to estimate power requirements, but this may be more complex if electro-reduction/electro-oxidation processes take place, which is ascertained with nitrate anions and Cr(VI) cations, among others. However, if adsorption or complexation is the prevailing
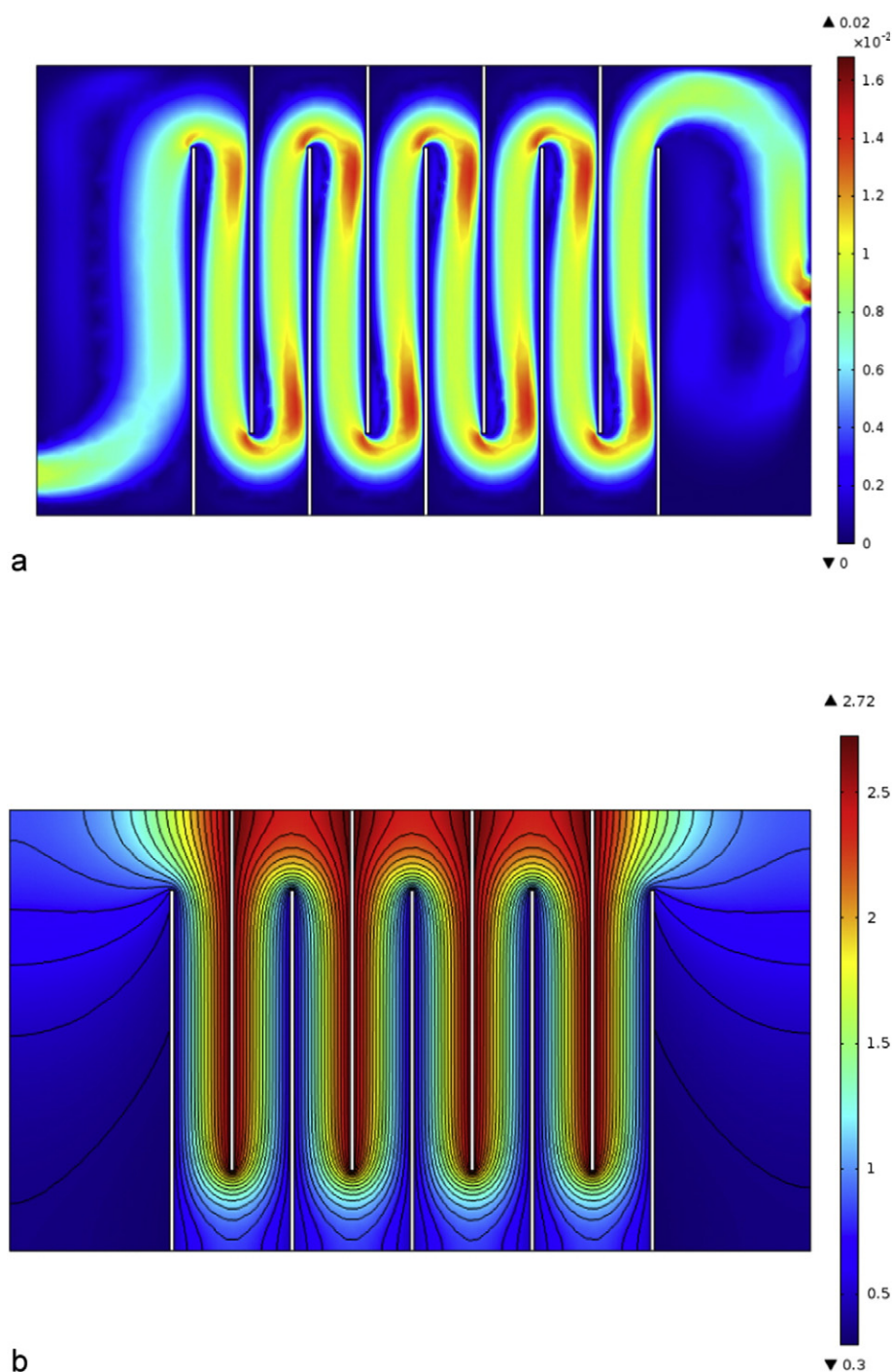
Fig. 9. a) Flow pattern b) velocity magnitude and secondary potential distributions throughout an EC cell at a flow rate 0.5 L min^{-1}.

mechanisms for pollution removal, only the amount of coagulant released is of utmost importance to estimate the removal yield.

Common adsorption and complexation models are usually based on the assumption of instantaneous equilibrium. Adsorption models present the advantage that they can use various adsorption isotherms, three of which are the most common: namely, Langmuir, Freundlich and Langmuir-Freundlich isotherm. Complexation models can more easily be applied to describe parallel mechanisms of pollution removal, as in the contribution model. However, only adsorption models have been applied as dynamic models, such as VOK, in which adsorption isotherm or adsorption kinetics can be combined to Faraday's law. A strong weakness of all these models is that they usually do not account for pH

evolution with time or space, respectively in batch and continuous EC cells.

In practice, flocculation modeling has been only hardly addressed. Smoluchowski's equation is the most common approach in the literature. This has been barely used in EC, first due to its unsuccessful application to real system, even though fractal dimension has been successfully used to elucidate the flocculation regime occurring during EC. Thus, this point deserves further investigation, as the effective pollution is achieved only after flocculation, followed by flotation or settling, which are also usually disregarded in EC modeling. CFD should be able to fill the gap between all these mechanisms because this method is able to account for the influence of hydrodynamics both on species

Table 5
Advantages and limitations of the different methods of EC modeling.

Model	Advantages	Limitations
RSM	Easy to couple with techno-economic or environmental analysis Very efficient for process optimization	Inadequate for scale-up No physical background Not efficient for process control
Phenomenological	Easy to use for scale-up purpose Analogy with kinetically-controlled chemical reactions	Poor fit with complex pollution Usually includes pseudo-kinetic constants Assumes perfect mixing and settling/flotation
Electrochemical	Estimation of power input and coagulant released Accounts for electro-oxidation/reduction	Prediction of a zeroth-order mechanism if no other limiting step (occurs usually only at short time) Assumption of perfect mixing and settling/flotation
Adsorption	Simple and versatile (isotherm) Analogy with conventional adsorption	Assumption of perfect settling/flotation Valid only if adsorption is governing Equilibrium assumed
Complexation	Simple and versatile (sequential/parallel reactions) Analogy with thermodynamically-controlled chemical reactions	Assumption of perfect settling/flotation Equilibrium assumed The complex mechanisms assumed do not necessarily describe the actual mechanism
VOK	Dynamic model Versatile: may account from equilibrium and kinetic limiting steps	Assumption of perfect settling/flotation One limiting step must be chosen
Flocculation/settling		Orthokinetic flocculation needs the description of hydrodynamics
CFD	Based on first principles Accounts for mixing and mass transfer, coupled with electrochemistry Adapted to scale-up purpose Correlations can be deduced for techno-economic analysis	Simulations may be time-consuming Influence of microbubbles and particles usually disregarded Flotation/settling models still to be coupled with hydrodynamics Coupling with cost estimation more complex than with simpler models

transport, orthokinetic flocculation for pollution removal and electrochemical phenomena. However, present research is still limited to the coupling between single-phase hydrodynamics and electrochemical processes, which means that further work is necessary to account for the formation of the solid phase, the role of hydrogen bubbles and the local change of pH during EC. Finally, the advantages and drawbacks of these methodologies for scale-up of EC process are summarized in Table 5.

5. Techno-economic evaluation of EC

A use of EC process in industry as a water/wastewater treatment process depends on its cost-effectiveness. An economic analysis of EC process would take into consideration fixed capital and operating costs [34]. The fixed capital cost comprises mainly the total purchase equipment cost (electrolytic cell, pumps) and the cost of their set up. The operating cost comprises mainly the costs of chemicals, electrodes and energy consumptions, but for an accurate cost evaluation of EC process, costs pertaining to labor, maintenance, sludge dewatering and disposal should be equally considered [122–124].

Operating costs OC as portrayed by Eq. (92) take into account major cost items including energy, electrode material, chemical costs and sludge handling costs. Besides the continuous EC system, batch EC system especially at industrial or pilot scale may use the pumps to feed the reactors in water or/and to outpour the treated wastewater from the reactor. For the accurate electrode material consumption, Faraday's law should take into consideration the electric current yield. Electrode material consumption and energy consumption are summarized in Table 6.

$$OC = aC + b\left(W + W'\right) + cK + dD \tag{92}$$

In Eq. (92), K (kg/m^3) measures the amount of chemicals consumed to treat 1 m^3 of water/wastewater, D (kg/m^3) is the sludge quantity generated by 1 m^3 of water/wastewater, and a ($/kg), c ($/kg), and d ($/kg) are electrode material unit price, unit price of chemicals and costs associated with sludge handling and disposal, respectively. Finally, b ($/kWh) is the electrical energy unit price per kWh. Maintenance cost can be reduced if current reversal between anode and cathode is applied.

Table 7 gives us a general insight on EC operating cost as a function of electrode material and electrode configuration and the comparison of operating cost of EC process with alternative treatments. Operating cost of EC using aluminum electrodes is higher than that using iron electrodes and this is due to their respective prices of each metal (about 0.5–0.8 US$/kg for iron and 1.5–3 US$/kg for aluminum). As for electrodes configuration, monopolar electrode configuration especially MP-P offers the high ratio of efficiency over operating cost thanks to its lower energy consumption. Overall EC is cost-effective process in comparison with other chemical processes. Even though the operating cost of both processes is of the same magnitude, disregarding the process efficiency, EC can be cheaper that chemical coagulation and vice versa depending on the range of current/current density used, but generally, when EC operates under lower current density, its operating cost is lower than that of chemical coagulation, as current is used as a chemical reactant. In addition, EC offers some advantages over chemical coagulation, such as the buffer effect that allows to avoid final acidic pH, the disinfection effect, the high removal efficiency of dissolved pollutants and the avoidance of some anions (SO_4^{2-}, Cl^-) usually added during chemical coagulation. Operating costs of chemical coagulation are composed of the cost of chemicals and the sludge handling and disposal. Considering that EC process is a low-sludge producing technique that does not use of additional chemicals with no secondary pollution, these operating expenses should be reduced when EC is used, as sludge composition and disposal procedures should be similar. However, maintenance costs may be higher with EC. Finally, in comparison with chemical coagulation, EC usually appears as an eco-friendly and cost-effective process, especially when it is operated below 20 mA/cm^2. In addition, sludge produced during EC is often less toxic than that in chemical coagulation, especially due to the lack of additive agents. However, sludge disposal may become an issue. In this case, recycling sludge or coagulant recovery from sludge could be an attractive option. Coagulant recovery can be achieved either by acidification or by alkalization; unfortunately, these can lead to the solubilization of pollutants contained in the sludge in addition to metal hydroxides [132,133]. Recycling may be more interesting. First, the sludge retrieved after EC process can be effectively used as a coagulant or as an adsorbent for subsequent wastewater treatment [134], provided adsorbed pollutants are not released. Otherwise, sludge can also be used as a building material.

As shown by Eq. (92), cost estimation requires a model describing electrodissolution, usually based on Faraday's law, another for the prediction of pollution removal, and an electrochemical model able to estimate electrical power consumption. For process design or optimization, this means that cost estimation is strongly coupled to removal yield and power input, i.e. to the models described in Section 4, with a constraint

Table 6

Calculation of electrode material and energy consumed during EC.

Mode	Material	Energy	
		Consumed by EC	Consumed by pumps
Batch	$C = \frac{M}{V}\frac{It}{ZF}$ (kg/m³)	$W = \frac{UI}{V}t$ (kWh/m³)	$W' = \frac{U'I'}{V}t$ (kWh/m³)
Continuous	$C = \frac{M}{Q}\frac{I}{ZF}$ (kg/m³)	$W = \frac{UI}{Q}$ (kWh/m³)	$W' = \frac{U'I'}{Q}$ (kWh/m³)

on the quality standards on either drinking water or industrial effluents. Techno-economic analysis is, therefore, easier for process optimization when RSM is used, as only analytical quadratic models are involved [80,129]. On the contrary, coupling economic analysis of EC with CFD has not been reported in the literature yet. This means that scale-up methods and techno-economic analysis are still difficult to couple, which explains why EC is not so popular for water treatment in comparison to chemical coagulation or biological processes. In practice, this means that optimum conditions found through RSM at laboratory

Table 7

Comparison of operating cost of EC, CC (chemical coagulation), CP (chemical precipitation) and (AD) adsorption processes (tst: ton of soil treated, CS: cocoa shell).

Pollutants wastewater (initial concentration)	Process/material	Removal efficiency	Specific energy consumed (current density)	Operating cost	Mode/reference
Synthetic wastewater (red dye (100 mg/L, pH 6.1))	Al-EC	80%–95%	1.5–3.5 kWh/kg dye (208–310 A/m²)	0.34–0.52 US$/kg dye	Continuous [125]
	CC	87%		0.32 US$/kg dye	
Synthetic wastewater (acid dye (50 mg/L, pH 7))	Al-EC	87.5–93.4%	27.8–99.0 kWh/kg dye (155–350 A/m²)	7.04–17.4 US$/kg dye (0.31–0.8 US$/m³)	Batch [47]
	Fe-EC	90.7–98.1%	26.7–76.6 kWh/kg dye (155–350 A/m²)	4.01–13.8 US$/kg dye (0.19–0.68 $/m³)	
Coal mine drainage wastewater (various metals)	Fe-EC	28.7–99.96%	1.32–5.6 kWh/m³ (200–500 A/m²)	1.09–2.184 US$/m³ (0.91–1.93 £/m³)	Batch [126]
	CP(NaOH)			1.173–7.49 US$/m³ (1.0364–6.6177 £/m³)	
Textile dye wastewater (3422 mg/LCOD)	Al-EC	15–62%	50–200 A/m²	0.32–0.58 US$/kg COD	Batch [34]
	Fe-EC	57–78%	50–200 A/m²	0.7–0.175 US$/kg COD	
Textile wastewater (2031 mg/L COD)	Al-EC(MP-P)		0.72–3 kWh/m³ (30–60 A/m²)	0.4–0.65 US$/m³	Batch [60]
	Al-EC(MP-S)		3–10 kWh/m³ (30–60 A/m²)	0.6–1.3 US$/m³	
	Al-EC(BP-S)		3.2–12.2 kWh/m³ (30–60 A/m²)	0.7–1.55 US$/m³	
	Fe-EC(MP-P)		0.68–2.5 kWh/m³ (30–60 A/m²)	0.25–0.4 US$/m³	
	Fe-EC(MP-S)		3–8.5 kWh/m³ (30–60 A/m²)	0.42–0.85 US$/m³	
	Fe-EC(BP-S)		3.3–12 kWh/m³ (30–60 A/m²)	0.46–1.08 US$/m³	
Comparison of EC and CC under their optimum conditions	Al-EC(MP-P)	63%	0.72 kWh/m³ (30 A/m²)	0.4 US$/m³	
	Fe-EC(MP-P)	65%	0.68 kWh/m³ (30 A/m²)	0.25 US$/m³	
	CC(FeCl₃·6H₂O)	71%		0.67 US$/m³	
	CC(Fe₂(SO4)₃·7H₂O)	68%		0.75 US$/m³	
	CC(AlCl₃·6H₂O)	68%		0.96 US$/m³	
	CC(Al₂(SO4)₃·18H₂O)	59%		0.75 US$/my	
Waste metal cutting fluids(3155 mg/L(TOC)17,312 mg/L(COD)) Under optimum conditions	Al-EC	93%(COD)	60 A/m²	0.036 US$/kg COD (0.768 US$/m³)	Batch [127]
		80% (TOC)		0.228 US$/kg TOC (0.768 US$/m³)	
	Fe-EC	92% (COD)	60 A/m²	0.023 US$/kg COD (0.479 $/m³)	
		82% (TOC)		0.144 US$/kg TOC (0.479 $/m³)	
Rinse water from zinc phosphate coating(phosphate and zinc) under continuous mode (flow rate 50–400 mL/min)	Al-EC	99.9–9.683% (PO₄³⁻)	13.75–4 kWh/m³ (60 A/m²)	14.5–4.2 US$/m³	Continuous [123]
		99.8–99.2% (Zn²⁺)	13.75–4 kWh/m³ (60 A/m²)	14.5–4.2 US$/m³	
	Fe-EC	99.6–85.5% (PO₄³⁻)	12.6–5.45 kWh/m³ (60 A/m²)	12.9–5.6 US$/m³	
		99.3–96.1% (Zn²⁺)			
12.6–5.45 kWh/m³(60 A/m²)	12.9–5.6 US$/m³				
Removal of Pb²⁺ and Zn²⁺ from acidic soil leachate	Fe-EC	99.4%(Zn²⁺) 99.7% (Pb²⁺)	18.5 kWh/tst (68 A/m²)	35.38 US$tst-1	Batch [128]
	CP(Ca(OH)₂)	98.9% (Zn²⁺) 99% (Pb²⁺)	88.7 kg Ca(OH)₂/tst	38.29 US$tst-1	
	CP(NaOH)	97.2% (Zn²⁺) 98.3% (Pb²⁺)	65 kg NaOH/tst	50.98 US$tst-1	
	AD (CS)	91.6% (Zn²⁺) 90.0% (Pb²⁺)	100 kg CS/tst	39.15 US$tst-1	

scale are not necessarily robust against scale-up and that Eq. (92) on OC per m^3 water does not ensure a constant pollution abatement in this case. In practice, attempts to couple models other than RSM to techno-economic analysis, and in particular scale-up models, lack in the literature. The authors hope that this review will stimulate further work in this field because this constitutes one of the main challenges that EC process has to face with, together with the improved theoretical modeling of the mechanisms of pollution abatement.

6. Closing remarks and perspectives

EC process is still the subject of an intensive research activity because of its various advantages: it is simple, low-cost, eco-friendly, versatile, efficient, and it is also a nonspecific technique, able to remove almost all types of pollutants simultaneously. In practice, current is the only operating parameter once pH/conductivity have been adjusted, which means that the design of the cell must be robust. Consequently, this design is complex, because it encompasses cell and electrode geometries, feed mode and mixing conditions, which may affect current density distribution, settling/flotation conditions, and, therefore, pollution removal. In the last decade, the applicability of EC for drinking water and wastewater treatment has spread considerably, and new applications including microalgae harvesting have become attractive in the last years. However, most of the investigations remain purely experimental or use statistical models (such as RSM) for optimization of operating conditions. While the open vertical-plate reactor remains the most common cell geometry, the A/V ratio and the electrode distance are still to be defined by a scale-up methodology, as well as the geometry of the separation section. Actually, the main weakness of this methodology is still the lack of understanding the interactions of different processes involved. Despite the various original modeling approaches developed in the last decade, such as VOK or complexation models, the link with flotation or settling efficiency, and a more general scale-up procedure is still to define for EC process. This means that no established methodology is able to address at the same time the prediction of pollution removal, settling/flotation, scale-up and techno-economic optimization and that subsequent developments in EC modeling are definitely necessary. Thus, CFD seems able to fill the gap between phenomenological models and knowledge-based models using correlations derived from CFD data, for example in techno-economic analysis. While electrochemistry has already been implemented in CFD codes that account for coupled hydrodynamic and mass transfer phenomena, this approach usually considers only single phase flows. Further work in this field must be encouraged, even though EC remains time- and CPU-expensive, which explains why it is used without considering the multiphase flow of EC. In addition, CFD deals with mixing, mass transfer and current distribution and is now able to model coagulation and floc growth using population balance models (PBE) already developed in other applications, such as bioreactors or chemical precipitation processes [130, 131]. However, the implementation of PBE is still limited in EC process because models able to account for flotation and/or coagulation/settling still require fundamental understanding and experimental data when an electric field is applied. This highlights that further work is necessary also in these fields because physical models able to describe accurately these phenomena have not been implemented in CFD codes yet. It is also probable that numerical issues will also have to be addressed when robust models will be defined. In addition, CFD must also be coupled to techno-economic analysis. Even though CFD will become easier to use with faster and more powerful computers in the future, two-phase or three-phase computations will remain expensive and the strategy of a techno-economic optimization strategy including CFD is still to define.

As a conclusion, even though EC is a robust and versatile process, it remains more difficult to simulate than other water treatments, such as biological processes. Further work is still necessary to achieve the same level of understanding and robustness in EC as in those alternative processes. As discussed above, two main research paths emerge from this review. The first one involves the application of CFD to EC cells that is still to be developed and must include more and more physics, and the second one aims the separation step of EC, by flotation or settling, in the presence of an electric that both requires experimental and theoretical analysis. The authors hope that this review paper will stimulate investigations in these fields.

Acknowledgments

References

[1] WHO, Global Analysis and Assessment of Sanitation and Drinking-Water (GLAAS), 2012 1–112.

[2] M.M. Emamjomeh, M. Sivakumar, Review of pollutants removed by electrocoagulation and electrocoagulation/flotation processes, J. Environ. Manag. 90 (2009) 1663–1679.

[3] I. Kabdaşı, I. Arslan-Alaton, T. Ölmez-Hanci, O. Tünay, Electrocoagulation applications for industrial wastewater: a critical review, Environ. Technol. Rev. 1 (2012) 2–45.

[4] P.K. Holt, G.W. Barton, C.A. Mitchell, The future for electrocoagulation as a localized water treatment technology, Chemosphere 59 (2005) 355–367.

[5] M.Y.A. Mollah, R. Schennach, J.R. Parga, D.L. Cocke, Electrocoagulation (EC)-science and applications, J. Hazard. Mater. B84 (2001) 29–41.

[6] P.K. Holt, Electrocoagulation: Unraveling and Synthesizing the Mechanisms behind a Water Treatment Process, The University of Sydney, 2002 (Thesis report).

[7] M. Kobya, O.T. Can, M. Bayramoglu, Treatment of textile wastewaters by electrocoagulation using iron and aluminum electrodes, J. Hazard. Mater. B100 (2003) 163–178.

[8] G. Mouedhen, M. Feki, M. De Petris Wery, H.F. Ayedi, Behavior of aluminum electrodes in electrocoagulation process, J. Hazard. Mater. 150 (2008) 124–135.

[9] X. Chen, G. Chen, P.L. Yue, Separation of pollutants from restaurant wastewater by electrocoagulation, Sep. Purif. Technol. 19 (2000) 65–76.

[10] W. Den, C.-J. Wang, Removal of silica from brackish water by electrocoagulation pretreatment to prevent fouling of reverse osmosis membranes, Sep. Purif. Technol. 59 (2008) 318–325.

[11] C.Y. Hu, S.L. Lo, W.H. Kuan, Simulation the kinetics of fluoride removal by electrocoagulation (EC) process using aluminum electrodes, J. Hazard. Mater. 145 (2007) 180–185.

[12] A. Bagga, S. Chellam, D.A. Clifford, Evaluation of iron chemical coagulation and electrocoagulation pretreatment for surface water microfiltration, J. Membr. Sci. 309 (2008) 82–93.

[13] Z. Gu, Z. Liao, M. Schulz, J.R. Davis, J.C. Baygents, J. Farrell, Estimating dosing rates and energy consumption for electrocoagulation using iron and aluminum electrodes, Ind. Eng. Chem. Res. 48 (2009) 3112–3117.

[14] K. Mansouri, K. Ibrik, N. Bensalaha, A. Abdel-Wahab, Anodic dissolution of pure aluminum during electrocoagulation process: influence of supporting electrolyte, initial pH, and current density, Ind. Eng. Chem. Res. 50 (2011) 13362–13372.

[15] M. Vepsäläinen, J. Selin, P. Rantala, M. Pulliainen, H. Särkkä, K. Kuhmonen, M. Sillanpää, Precipitation of dissolved sulphide in pulp and paper mill wastewater by electrocoagulation, Environ. Technol. 32 (2011) 1393–1400.

[16] A. De Mello Ferreira, M. Marchesiello, P.X. Thivel, Removal of copper, zinc and nickel present in natural water containing Ca^{2+} and HCO$_3^-$ ions by electrocoagulation, Sep. Purif. Technol. 107 (2013) 109–117.

[17] E. Lacasa, P. Canizares, C. Sáez, F.J. Fernández, M.A. Rodrigo, Electrochemical phosphates removal using iron and aluminium electrodes, Chem. Eng. J. 172 (2011) 137–143.

[18] A.K. Golder, A.N. Samanta, S. Ray, Removal of phosphate from aqueous solutions using calcined metal hydroxides sludge waste generated from electrocoagulation, Sep. Purif. Technol. 52 (2006) 102–109.

[19] M. Rehbun, M. Lurie, Control of organic matter by coagulation and flocculation separation, Water Sci. Technol. 27 (1993) 1–20.

[20] J. Zhu, H. Zhao, J. Ni, Fluoride distribution in electrocoagulation defluoridation process, Sep. Purif. Technol. 56 (2007) 184–191.

[21] M.M. Emamjomeh, M. Sivakumar, A.S. Varyani, Analysis and the understanding of fluoride removal mechanisms by an electrocoagulation/flotation (ECF) process, Desalination 275 (2011) 102–106.

[22] C.Y. Hu, S.L. Lo, W.H. Kuan, High concentration of arsenate removal by electrocoagulation with calcium, Sep. Purif. Technol. 126 (2014) 7–14.

[23] I. Zongo, J.P. Leclerc, H.A. Maiga, J. Wéthé, F. Lapicque, Removal of hexavalent chromium from industrial wastewater by electrocoagulation: a comprehensive comparison of aluminium and iron electrodes, Sep. Purif. Technol. 66 (2009) 159–166.

[24] M.M. Emamjomeh, M. Sivakumar, Denitrification using a monopolar electrocoagulation/flotation (ECF) process, J. Environ. Manag. 91 (2009) 516–522.

[25] P.R. Kumar, S. Chaudhari, K.C. Khilar, S.P. Mahajan, Removal of arsenic from water by electrocoagulation, Chemosphere 55 (2004) 1245–1252.

[26] B. Al Aji, Y. Yavuz, A.S. Koparal, Electrocoagulation of heavy metals containing model wastewater using monopolar iron electrodes, Sep. Purif. Technol. 86 (2012) 248–254.

[27] C.Y. Hu, S.L. Loa, W.H. Kuan, Effects of co-existing anions on fluoride removal in electrocoagulation (EC) process using aluminum electrodes, Water Res. 37 (2003) 4513–4523.

[28] J. Duan, J. Gregory, Coagulation by hydrolyzing metal salts, Adv. Colloid Interf. Sci. 100-102 (2003) 475–502.

[29] Y. Liang, N. Hilal, P. Langston, V. Starov, Interaction forces between colloidal particles in liquid: theory and experiment, Adv. Colloid Interf. Sci. 134-135 (2007) 151–166.

[30] T. Harif, M. Khai, A. Adin, Electrocoagulation versus chemical coagulation: coagulation/ flocculation mechanisms and resulting floc characteristics, Water Res. 46 (2012) 3177–3188.

[31] P. Cañizares, F. Martínez, M.A. Rodrigo, C. Jiménez, C. Sáez, J. Lobato, Modeling of wastewater electrocoagulation processes part I. General description and application to kaolin-polluted wastewaters, Sep. Purif. Technol. 60 (2008) 155–161.

[32] M.Y.A. Mollah, P. Morkovsky, J.A.G. Gomes, M. Kesmez, J. Parga, D.L. Cocke, Fundamentals, present and future perspectives of electrocoagulation, J. Hazard. Mater. B114 (2004) 199–210.

[33] T. Harif, A. Adin, Size and structure evolution of kaoline Al(OH)$_3$ flocs in the electroflocculation process: a study using static light scattering, Water Res. 45 (2011) 6195–6206.

[34] M. Bayramoglu, M. Kobya, O.T. Can, M. Sozbir, Operating cost analysis of electrocoagulation of textile dye wastewater, Sep. Purif. Technol. 37 (2004) 117–125.

[35] O.T. Can, M. Bayramoglu, M. Kobya, Decolorization of reactive dye solutions by electrocoagulation using aluminum electrodes, Ind. Eng. Chem. Res. 42 (2003) 3391–3396.

[36] M. Kobya, H. Hiz, E. Senturk, C. Aydiner, E. Demirbas, Treatment of potato chips manufacturing, Desalination 190 (2006) 201–211.

[37] A. Akyol, Treatment of paint manufacturing wastewater by electrocoagulation, Desalination 285 (2012) 91–99.

[38] H.K. Hansen, P. Nuñez, D. Raboy, I. Schippacasse, R. Grandon, Electrocoagulation in wastewater containing arsenic: comparing different process designs, Electrochim. Acta 52 (2007) 3464–3470.

[39] C. Comninellis, G. Chen, Electrochemistry for the Environment, Springer Science + Business Media, LLC, 2010.

[40] N. Mameri, A.R. Yeddou, H. Lounici, D. Belhicine, H. Grid, B. Bariou, Defluoridation of septentrional Sahara water of North Africa by electrocoagulation process using bipolar aluminium electrodes, Water Res. 32 (5) (1998) 1604–1612.

[41] M. Ben Sasson, W. Calmano, A. Adin, Iron-oxidation processes in an electroflocculation (electrocoagulation) cell, J. Hazard. Mater. 171 (2009) 704–709.

[42] C. Jiménez, C. Sáez, F. Martínez, P. Cañizares, M.A. Rodrigo, Electrochemical dosing of iron and aluminum in continuous processes: a key step to explain electro-coagulation processes, Sep. Purif. Technol. 98 (2012) 102–108.

[43] M. Malakootian, H.J. Mansoorian, M. Moosazadeh, Performance evaluation of electrocoagulation process using iron-rod electrodes for removing hardness from drinking water, Desalination 255 (2010) 67–71.

[44] D. Lakshmanan, D.A. Clifford, G. Samanta, Ferrous and ferric ion generation during iron electrocoagulation, Environ. Sci. Technol. 43 (2009) 3853–3859.

[45] K. Mansouri, K. Elsaid, A. Bedoui, N. Bensalaha, A. Abdel-Wahab, Application of electrochemically dissolved iron in the removal of tannic acid from water, Chem. Eng. J. 172 (2011) 970–976.

[46] M. Kobya, E. Senturk, M. Bayramoglu, Treatment of poultry slaughterhouse wastewaters by electrocoagulation, J. Hazard. Mater. 133 (2006) 172–176.

[47] M. Chafi, B. Gourich., A.H. Essadki, C. Vial, A. Fabregat, Comparison of electrocoagulation using iron and aluminium electrodes with chemical coagulation for the removal of a highly soluble acid dye, Desalination 281 (2011) 285–292.

[48] Y. Gendel, O. Lahav, A new approach to increasing the efficiency of low-pH Fe-electrocoagulation applications, J. Hazard. Mater. 183 (2010) 596–601.

[49] P.K. Holt, G.W. Barton, M. Wark, C.A. Mitchell, A quantitative comparison between chemical dosing and electrocoagulation, Colloids Surf. A Physicochem. Eng. Asp. 211 (2002) 233–248.

[50] T. Harif, A. Adin, Characteristics of aggregates formed by electroflocculation of a colloidal suspension, Water Res. 41 (2007) 2951–2961.

[51] I. Zongo, Étude expérimentale et théorique du procédé d'électrocoagulation, application du traitement de deux effluents textiles et d'un effluent simulé de tannerie, Institut National Polytechnique de Lorraine, 2009 (PhD thesis report).

[52] A.S. Koparal, Ü.B. Ögütveren, Removal of nitrate from water by electroreduction and electrocoagulation, J. Hazard. Mater. B89 (2002) 83–94.

[53] L. Fan, Y. Zhou, W. Yang, G. Chen, F. Yang, Electrochemical degradation of aqueous solution of Amaranth azo dye on ACF under potentiostatic model, Dyes Pigments 76 (2008) 440–446.

[54] L.A.M. Ruotolo, J.C. Gubulin, A mathematical model to predict the electrode potential profile inside a polyaniline-modified reticulate vitreous carbon electrode operating in the potentiostatic reduction of Cr(VI), Chem. Eng. J. 171 (2011) 1170–1177.

[55] D. Ghosh, H. Solanki, M.K. Purkait, Removal of Fe(II) from tap water by electrocoagulation technique, J. Hazard. Mater. 155 (2008) 135–143.

[56] O. Larue, E. Vorobiev, C. Vub, B. Durand, Electrocoagulation and coagulation by iron of latex particles in aqueous suspensions, Sep. Purif. Technol. 31 (2003) 177–192.

[57] G. Chen, Electrochemical technologies in wastewater treatment, Sep. Purif. Technol. 38 (2004) 11–41.

[58] H.Z. Zhao, W. Yang, J. Zhu, J.R. Ni, Defluoridation of drinking water by combined electrocoagulation: effects of the molar ratio of alkalinity and fluoride to Al(III), Chemosphere 74 (2009) 1391–1395.

[59] A. de Mello Ferreira, M. Marchesiello, P.-X. Thivel, Removal of copper, zinc and nickel present in natural water containing Ca^{2+} and HCO^{3-} ions by electrocoagulation, Sep. Purif. Technol. 107 (2013) 109–117.

[60] M. Bayramoglu, M. Eyvaz, M. Kobya, Treatment of the textile wastewater by electrocoagulation: economical evaluation, Chem. Eng. J. 128 (2007) 155–161.

[61] A.K. Golder, A.N. Samanta, S. Ray, Removal of Cr^{3+} by electrocoagulation with multiple electrodes: bipolar and monopolar configurations, J. Hazard. Mater. 141 (2007) 653–661.

[62] M. Kobya, F. Ulu, U. Gebologlu, E. Demirbas, M.S. Oncel, Treatment of potable containing low concentration of arsenic with electrocoagulation: different connections mode and Fe-Al electrodes, Sep. Purif. Technol. 77 (2011) 283–293.

[63] C.T. Wang, W.L. Chou, Y.M. Kuo, Removal of COD from laundry wastewater by electrocoagulation/electroflotation, J. Hazard. Mater. 164 (2009) 81–86.

[64] P. Drogui, M. Asselin, S.K. Brar, H. Benmoussa, J.F. Blais, Electrochemical removal of pollutants from agro-industry wastewaters, Sep. Purif. Technol. 61 (2008) 301–310.

[65] J.Q. Jiang, N. Graham, C. André, G.H. Kelsall, B. Nigel, Laboratory study of electro-coagulation-flotation for water treatment, Water Res. 36 (2002) 4064–4078.

[66] N. Modirshahla, M.A. Behnajady, S. Kooshaiian, Investigation of the effect of different electrode connections on the removal efficiency of Tartrazine from aqueous solutions by electrocoagulation, Dyes Pigments 74 (2007) 249–257.

[67] Y.O.A. Fouad, A.H. Konsowa, H.A. Farag, G.H. Sedahmed, Performance of an electrocoagulation cell with horizontally oriented electrodes in oil separation compared to a cell with vertical electrodes, Chem. Eng. J. 145 (2009) 436–440.

[68] J.F. Martínez-Villafañe, C. Montero-Ocampo, A.M. García-Lara, Energy and electrode consumption analysis of electrocoagulation for the removal of arsenic from underground water, J. Hazard. Mater. 172 (2009) 1617–1622.

[69] S. Zhang, J. Zhang, W. Wang, F. Li, X. Cheng, Removal of phosphate from landscape water using an electrocoagulation process powered directly by photovoltaic solar modules, Sol. Energy Mater. Sol. Cells 117 (2013) 73–80.

[70] M. Al-Shannag, Z. Al-Qodah, K. Bani-Melhem, M.R. Qtaishat, M. Alkasrawi, Heavy metal ions removal from metal plating wastewater using electrocoagulation: kinetic study and process performance, Chem. Eng. J. 260 (2015) 749–756.

[71] B. Merzouk, B. Gourich, A. Sekki, K. Madani, C. Vial, M. Barkaoui, Studies on the decolorization of textile dye wastewater by continuous electrocoagulation process, Chem. Eng. J. 149 (2009) 207–214.

[72] A.H. Essadki, M. Bennajah, B. Gourich, C. Vial, M. Azzi, H. Delmas, Electrocoagulation/electroflotation in an external-loop airlift reactor/application to the decolorization of textile dye wastewater: a case study, Chem. Eng. Process. 47 (2008) 1211–1223.

[73] WHO's drinking water standards 1993.

[74] W.L. Chou, Removal and adsorption characteristics of polyvinyl alcohol from aqueous solutions using electrocoagulation, J. Hazard. Mater. 177 (2010) 842–850.

[75] M. Tir, N. Moulai-Mostef, Optimization of oil removal from oily wastewater by electrocoagulation using response surface method, J. Hazard. Mater. 158 (2008) 107–115.

[76] W.-J. Chen, W.-T. Su, H.-Y. Hsu, Continuous flow electrocoagulation for MSG wastewater treatment using polymer coagulants via mixture-process design and response-surface methods, J. Taiwan Inst. Chem. Eng. 43 (2012) 246–255.

[77] R. Daghrir, P. Drogui, F. Zaviska, Effectiveness of a hybrid process combining electro-coagulation and electro-oxidation for the treatment of domestic wastewaters using response surface methodology, J. Environ. Sci. Health A 48 (2013) 308–318.

[78] K. Kishor Garg, B. Prasad, Treatment of multicomponent aqueous solution of purified terephthalic acid wastewater by electrocoagulation process: optimization of process and analysis of sludge, J. Taiwan Inst. Chem. Eng. 60 (2016) 383–393.

[79] A.R. Amani-Ghadim, S. Aber, A. Olad, H. Ashassi-Sorkhabi, Optimization of electrocoagulation process for removal of an azo dye using response surface methodology and investigation on the occurrence of destructive side reactions, Chem. Eng. Process. 64 (2013) 68–78.

[80] E. Gengec, M. Kobya, E. Demirbas, A. Akyol, K. Oktor, Optimization of baker's yeast wastewater using response surface methodology by electrocoagulation desalination, Water Air Soil Pollut. 286 (2012) 200–209.

[81] T. Olmez-Hanci, Z. Kartal, I. Arslan-Alaton, Electrocoagulation of commercial naphthalene sulfonates: process optimization and assessment of implementation potential, J. Environ. Manag. 99 (2012) 44–51.

[82] M.S. Bhatti, A.S. Reddy, A.K. Thukral, Electrocoagulation removal of Cr(VI) from simulated wastewater using response surface methodology, J. Hazard. Mater. 172 (2009) 839–846.

[83] M.S. Bhatti, A.S. Reddy, R.K. Kalia, A.K. Thukral, Modeling and optimization of voltage and treatment time for electrocoagulation removal of hexavalent chromium, Desalination 269 (2011) 157–162.

[84] O. Chavalparit, M. Ongwandee, Optimizing electrocoagulation process for the treatment of biodiesel wastewater using response surface methodology, J. Environ. Sci. 21 (2009) 1491–1496.

[85] S. Zodi, O. Potier, F. Lapicque, J.-P. Leclerc, Treatment of the industrial wastewaters by electrocoagulation: optimization of coupled electrochemical and sedimentation processes, Desalination 261 (2010) 186–190.

[86] K.K. Garg, B. Prasad, Development of box Behnken design for treatment of terephthalic acid wastewater by electrocoagulation process: optimization of process and analysis of sludge, J. Environ. Chem. Eng. 4 (2016) 178–190.

[87] B.-Y. Tak, B.-S. Tak, Y.-J. Kim, Y.-J. Park, Y.-H. Yoon, G.-H. Min, Optimization of color and COD removal from livestock wastewater by electrocoagulation process: application of box–Behnken design (BBD), J. Ind. Eng. Chem. 28 (2015) 307–315.

[88] M. Vepsäläine, M. Ghiasvand, J. Selinc, J. Pienimaa, E. Rep, M. Pulliainen, M. Sillanpää, Investigations of the effects of temperature and initial sample pH on natural organic matter (NOM) removal with electrocoagulation using response surface method (SRM), Sep. Purif. Technol. 69 (2009) 255–261.

[89] Z. Zaroual, H. Chaair, A.H. Essadki, K. El Ass, M. Azzi, Optimizing the removal of trivalent chromium by electrocoagulation using experimental design, Chem. Eng. J. 148 (2009) 488–495.

[90] T. Yehya, M. Chafi, W. Balla, C. Vial, A. Essadki, B. Gourich, Experimental analysis and modeling of denitrification using electrocoagulation process, Sep. Purif. Technol. 132 (2014) 644–654.

[91] A. Shafaei, E. Pajootan, M. Nikazar, M. Arami, Removal of Co (II) from aqueous solution by electrocoagulation process using aluminum electrodes, Desalination 279 (2011) 121–126.

[92] A. Shafaei, M. Rezaie, M. Nikazar, Evaluation of Mn^{2+} and Co^{2+} removal by electrocoagulation: a case study, Chem. Eng. Process. 50 (2011) 1115–1121.

[93] M.M. Emamjomeh, M. Sivakumar, An empirical model for defluoridation by batch monopolar electrocoagulation/flotation (ECF) process, J. Hazard. Mater. B131 (2006) 118–125.

[94] A.H. Essadki, B. Gourich, M. Azzi, C. Vial, H. Delmas, Kinetic study of defluoridation of drinking water by electrocoagulation/electroflotation in a stirred tank reactor and in an external-loop airlift reactor, Chem. Eng. J. 164 (2010) 106–114.

[95] W.L. Chou, C.T. Wang, K.Y. Huang, Investigation of process parameters for the removal of polyvinyl alcohol from aqueous solution by iron electrocoagulation, Desalination 251 (2010) 12–19.

[96] E.A. Yılmaza, R. Boncukcuoğlu, M.M. Kocakerim, E. Kocadağistan, An empirical model for kinetics of boron removal from boron containing wastewaters by the electrocoagulation method in a batch reactor, Desalination 230 (2008) 288–297.

[97] X. Chen, G. Chen, P.L. Yue, Investigation on the electrolysis voltage of electrocoagulation, Chem. Eng. Sci. 57 (2002) 2449–2455.

[98] K.L. Dubrawski, C. Du, M. Mohseni, General potential-current model and validation for electrocoagulation, Electrochim. Acta 129 (2014) 187–195.

[99] N. Balasubramanian, T. Kojima, C. Srinivasakannan, Arsenic removal through electrocoagulation: kinetic and statistical modeling, Chem. Eng. J. 155 (2009) 76–82.

[100] W.L. Chou, C.T. Wang, W.C. Chang, S.Y. Chang, Adsorption treatment of oxide chemical mechanical polishing wastewater from a semiconductor manufacturing plant by electrocoagulation, J. Hazard. Mater. 180 (2010) 217–224.

[101] W.L. Chou, C.T. Wang, K.Y. Huang, T.C. Li, Electrochemical removal of salicylic acid from aqueous solutions using aluminum electrodes, Desalination 271 (2011) 55–61.

[102] V. Khatibikamala, A. Torabiana, F. Janpoora, G. Hoshyaripourb, Fluoride removal from industrial wastewater using electrocoagulation and its adsorption kinetics, J. Hazard. Mater. 179 (2010) 276–280.

[103] Z.V.P. Murthy, S. Parmar, Removal of strontium by electrocoagulation using stainless steel and aluminum electrodes, Desalination 282 (2011) 63–67.

[104] S. Vasudevan, J. Lakshmi, G. Sozhan, Studies on the Al–Zn–In-alloy as anode material for the removal of chromium from drinking water in electrocoagulation process, Desalination 275 (2011) 260–268.

[105] D.N. Thomas, S.J. Judd, N. Fawcett, Flocculation modelling: a review, Water Res. 33 (1999) 1579–1592.

[106] G.C. Bushell, Y.D. Yan, D. Woodfield, J. Raper, R. Amal, On techniques for the measurement of the mass fractal dimension of aggregates, Adv. Colloid Interf. Sci. 95 (2002) 1–50.

[107] P. Tang, J.A. Raper, Modelling the settling behaviour of fractal aggregates: a review, Powder Technol. 123 (2002) 114–125.

[108] A. Vahedi, B. Gorczyca, Application of fractal dimensions to study the structure of flocs formed in lime softening process, Water Res. 45 (2011) 545–556.

[109] E. Ofir, Y. Oren, A. Adin, Modified equilibrium-solubility domains and a kinetic model of iron oxide and hydroxide colloids for lector flocculation, Desalination 204 (2007) 79–86.

[110] L.L. Chen, H.L. Sheng, Treatment of chemical mechanical polishing wastewater by electrocoagulation: system performances and sludge settling characteristics, Chemosphere 54 (2004) 235–242.

[111] S. Zodi, O. Potier, F. Lapicque, J.P. Leclerc, Treatment of the textile wastewaters by electrocoagulation: effect of operating parameters on the sludge settling characteristics, Sep. Purif. Technol. 69 (2009) 29–36.

[112] M. Khemis, J.P. Leclerc, G. Tanguy, G. Valentin, F. Lapicque, Treatment of industrial liquid wastes by electrocoagulation: experimental investigations and an overall interpretation model, Chem. Eng. Sci. 61 (2006) 3602–3609.

[113] I. Zongo, A.H. Maigab, J. Wéthéb, G. Valentin, J.P. Leclerc, G. Paternotte, F. Lapicque, Electrocoagulation for the treatment of textile wastewaters with Al or Fe electrodes: compared variations of COD levels, turbidity and absorbance, J. Hazard. Mater. 169 (2009) 70–76.

[114] B. Merzouk, M. Yakoubi, I. Zongo, J.P. Leclerc, G. Paternotte, S. Pontvianne, F. Lapicque, Effect of modification of textile wastewater composition on electrocoagulation efficiency, Desalination 275 (2011) 181–186.

[115] A. Vázquez, I. Rodríguez, I. Lázaro, Primary potential and current density distribution analysis: a first approach for designing electrocoagulation reactors, Chem. Eng. J. 179 (2012) 253–261.

[116] A. Vázquez, J.L. Nava, R. Cruz, I. Lázaro, I. Rodríguez, The importance of current distribution and cell hydrodynamic analysis for the design of electrocoagulation reactors, J. Chem. Technol. Biotechnol. 89 (2014) 220–229.

[117] S.M. Delgadillo, H.M. Ponce, V.M. Escamilla, C.G. Torres, J.J. Bernal, C.B. Diaz, Performance evaluation of an electrochemical reactor used to reduce Cr(VI) from aqueous media applying CFD simulations, J. Clean. Prod. 34 (2012) 120–124.

[118] H.K. Versteeg, W. Malalasekera, An Introduction to Computational Fluid Dynamics: The Finite Volume Method, Longman, London, 1995.

[119] F. Coeuret, A. Storck, Elément de Génie Electrochimique, Technique et Documentation, Paris, 1984.

[120] J.S. Newman, Electrochemical Systems, Prentice-Hall, London-Englewood Cliffs, 1973.

[121] H. Azargoshasb, S.M. Mousavi, T. Amani, A. Jafari, M. Nosrati, Three-phase CFD simulation coupled with population balance equations of anaerobic syntrophic acidogenesis and methanogenesis reactions in a continuous stirred bioreactor, J. Ind. Eng. Chem. 27 (2015) 207–217.

[122] T. Olmez-Hanci, Z. Kartal, I. Arslan-Alaton, Electrocoagulation of commercial naphthalene sulfonates: process optimization and assessment of implementation potential, J. Environ. Manag. 99 (2012) 44–51.

[123] M. Kobya, E. Demirbas, A. Dedeli, M.T. Sensoy, Treatment of rinse water from zinc phosphate coating by batch and continuous electrocoagulation processes, J. Hazard. Mater. 173 (2010) 326–334.

[124] M. Kobya, E. Gengec, E. Demirbas, Operating parameters and costs assessments of a real dyehouse wastewater effluent treated by a continuous electrocoagulation process, Chem. Eng. Process. 101 (2016) 87–100.

[125] B. Merzouk, B. Gourich, K. Madani, C. Vial, A. Sekki, Removal of a disperse red dye from synthetic wastewater by chemical coagulation and continuous electrocoagulation. A comparative study, Desalination 272 (2011) 246–253.

[126] M.S. Oncel, A. Muhcu, E. Demirbas, M. Kobya, A comparative study of chemical precipitation and electrocoagulation for treatment of coal acid drainage wastewater, J. Environ. Chem. Eng. 1 (2013) 989–995.

[127] M. Kobya, C. Ciftci, M. Bayramoglu, M.T. Sensoy, Study on the treatment of waste metal cutting fluids using electrocoagulation, Sep. Purif. Technol. 60 (2008) 285–291.

[128] P. Drogui, N. Meunier, G. Mercier, J.F. Blais, Removal of Pb^{2+} and Zn^{2+} ions from acidic soil leachate: a comparative study between electrocoagulation, adsorption and chemical precipitation processes, Int. J. Environ. Waste Manag. 8 (2011) (Nos 3/4).

[129] M. Behbahani, M.R. Alavi Moghaddam, M. Arami, Techno-economical evaluation of fluoride removal by electrocoagulation process: optimization through response surface methodology, Desalination 271 (2011) 209–218.

[130] E. Bartolini, H. Manoli, E. Costamagna, H.A. Jeyaseelan, M. Hamad, M.R. Irhimeh, A. Khademhosseini, A. Abbas, Population balance modelling of stem cell culture in 3D suspension bioreactors, Chem. Eng. Res. Des. 101 (2015) 125–134.

[131] P.Ş. Agachi, R. Barabás, B.G. Lakatos, Coupled population balance-CFD modelling of a continuous precipitation reactor, Comput. Aided Chem. Eng. 33 (2014) 187–192.

[132] A.M. Evuti, M. Lawal, Recovery of coagulants from water works sludge: a review, Adv. Appl. Sci. Res. 2 (6) (2011) 410–417.

[133] J. Keeley, P. Jarvis, A.D. Smith, S.J. Jud, Coagulant recovery and reuse for drinking water treatment, Water Res. 88 (2016) 502–509.

[134] S. Sadri Moghaddam, M.R. Alavi Moghaddam, M. Arami, Coagulation/flocculation process for dye removal using sludge from water treatment plant: optimization through response surface methodology, J. Hazard. Mater. 175 (2010) 651–657.